

See discussions, stats, and author profiles for this publication at: <https://www.researchgate.net/publication/392474225>

# Light at night negatively affects mood in diurnal primate-like tree shrews via a visual pathway related to the perihabenular nucleus

Article in *Proceedings of the National Academy of Sciences* · June 2025

DOI: 10.1073/pnas.2411280122

CITATIONS

0

READS

40

14 authors, including:



Huan Zhao

hefei university

28 PUBLICATIONS 1,245 CITATIONS

[SEE PROFILE](#)



Rui Bi

Chinese Academy of Sciences

69 PUBLICATIONS 1,516 CITATIONS

[SEE PROFILE](#)



Hongli Li

State Key Laboratory of Genetic Resources and Evolution, Kunming Institute of Zo...

29 PUBLICATIONS 587 CITATIONS

[SEE PROFILE](#)



Kai An

University of Science and Technology of China

4 PUBLICATIONS 439 CITATIONS

[SEE PROFILE](#)



# Light at night negatively affects mood in diurnal primate-like tree shrews via a visual pathway related to the perihabenular nucleus

Ying Miao<sup>a,b,1</sup> , Huan Zhao<sup>c,1,2</sup> , Yu-Fei Li<sup>a,1</sup> , Yan-Ping Sun<sup>a</sup>, Rui Bi<sup>b,d,e</sup> , Hongli Li<sup>b,d</sup> , Xin Fang<sup>a</sup> , Zi-Shuo Li<sup>a</sup> , Yu-Hua Ma<sup>d</sup> , Long-Bao Lv<sup>b,d</sup>, Kai An<sup>a</sup> , Jian-Jun Meng<sup>a,2</sup> , Yong-Gang Yao<sup>b,d,e,2</sup> , and Tian Xue<sup>a,2</sup>

Affiliations are included on p. 11.

Edited by Michael Tri H. Do, Boston Children's Hospital F M Kirby Neurobiology Center, Boston, MA; received June 6, 2024; accepted April 24, 2025 by Editorial Board Member Jeremy Nathans

To better understand the potential health threats and underlying visual pathways of long-term light at night (LAN) exposure, we adopted a widely accepted diurnal animal model tree shrew (*Tupaia belangeri chinensis*), which is a close relative to primates, and evaluated the deleterious effects of long-term LAN exposure. We used an early-night LAN paradigm that was established in mice to examine behavioral and physiological consequences in adult male tree shrews. We found that 3-wk LAN exposure significantly impaired the mood and long-term memory of tree shrews without affecting the general activity pattern. We identified retinal projections to the perihabenular nucleus (pHb), a crucial area in LAN-induced negative mood, and demonstrated that the pHb continues to innervate the nucleus accumbens (NAc) in tree shrews. Moreover, the pHb was required for the LAN effect on mood but not long-term memory. Transcriptomic profiling of brain tissues containing the NAc area revealed drastic changes of several depression-related genes in NAc neurons post-LAN treatment, suggesting that long-term exposure to nighttime light could result in lasting changes in tree shrews. Collectively, we present behavioral and neural structural evidence that LAN exerts depression-inducing effects in diurnal animals via a pHb-related visual pathway, which may facilitate the translation from laboratory findings of excessive LAN exposure to clinical applications in humans.

diurnal tree shrew | light at night | neural circuit | negative mood | long-term memory

Light is a salient environmental factor for life on earth, most naturally occurring in the form of sunlight. Photic cycles with alternating presence (day) and absence (night) of sunlight are internalized as biological rhythms in virtually all organisms (1–3), which exert a profound impact on numerous aspects of physiology (4–8). In addition to being the most prominent “zeitgeber” (the entraining agent) of the circadian rhythm, light also modulates various physiological processes via direct neural pathways (9–12), allowing organisms to precisely respond and adjust to the outside world. The invention and ever-growing usage of electric light and many light-emitting devices since the past century have introduced drastic changes to our light environment, especially at nighttime. Artificial light at night (LAN), though societally beneficial, has been strongly implicated as a risk factor for metabolic disorders, breast cancer, and endocrine and immune dysfunction, to name a few, by both human observational studies and animal research (13–17). LAN also has mostly adverse effects on mood and cognitive functions in humans, as suggested by a compelling body of epidemiological data (18–20), which urges experimental studies to provide a deeper understanding on health threats imposed by the rapidly increasing prevalence of LAN.

Studies using animal models, such as our previous work and others, have begun to reveal the neural mechanisms responsible for the effects of LAN on mood-related behaviors (11, 21–23). Specifically, we previously reported that chronic exposure to 2-h LAN induced depressive-like behaviors in C57BL/6 mice via a circadian-gated retina-perihabenular nucleus (pHb)-nucleus accumbens (NAc) pathway (22). However, when considering the translation of laboratory findings to strategies against LAN-imposed health problems in humans, one has to take into account that most existing knowledge regarding the structures and functional features of central pathways underlying the effects of LAN is obtained from nocturnal rodents. Although the “master clock” of the circadian rhythm, namely the suprachiasmatic nucleus (SCN), functions in a largely similar manner between nocturnal and diurnal species (24, 25), there remains pronounced behavioral, cellular, and

## Significance

Long-term light at night (LAN) exposure poses a health threat to nocturnal lab animals. Whether diurnal animals suffer the same deleterious effect imposed by LAN and how it works are still open questions. Our study shows that tree shrew, a primate-like diurnal animal, presents impaired mood and cognitive functions upon 3-wk LAN exposure. This effect is mediated by a conserved retina-perihabenular nucleus (pHb)-nucleus accumbens (NAc) pathway. Our findings constitute the basis for translational work aiming to prevent or treat mood disorders associated with excessive LAN.

Author contributions: H.Z., Y.-G.Y., and T.X. designed research; Y.M., Y.-F.L., R.B., H.L., X.F., Z.-S.L., Y.-H.M., L.-B.L., K.A., and J.-J.M. performed research; Y.M., H.Z., and Y.-P.S. analyzed data; and Y.M., H.Z., Y.-G.Y., and T.X. wrote the paper.

The authors declare no competing interest.

This article is a PNAS Direct Submission. M.T.H.D. is a guest editor invited by the Editorial Board.

Copyright © 2025 the Author(s). Published by PNAS. This article is distributed under Creative Commons Attribution-NonCommercial-NoDerivatives License 4.0 (CC BY-NC-ND).

<sup>1</sup>Y.M., H.Z., and Y.-F.L. contributed equally to this work.

<sup>2</sup>To whom correspondence may be addressed. Email: hzhao@hfuu.edu.cn, jianjunm@ustc.edu.cn, yaoyg@mail.kiz.ac.cn, or xuetian@ustc.edu.cn.

This article contains supporting information online at <https://www.pnas.org/lookup/suppl/doi:10.1073/pnas.2411280122/-DCSupplemental>.

Published June 6, 2025.

molecular distinctions between those two chronotypes (26, 27). Therefore, it is highly desirable to include diurnal animal models in the study of LAN effects to cross-examine the relevance of current understanding to human physiology, and in particular, to evaluate better whether in diurnal animals, including humans, LAN may work through similar evolutionarily conserved neural mechanisms.

A few attempts have been made to establish diurnal models for investigating the effects of LAN on mood, including studies with diurnal rodents, birds, and tree shrews (23, 28, 29). Most of these studies employed a dLAN (dim LAN) paradigm where dim light (5 to 10 lx) was present throughout the inactive period, and monitored outcomes at the behavioral and molecular levels. However, the neural mechanism, the exact central circuit in particular, which is responsible for the LAN-induced negative effects in diurnal animals remains unknown.

To address this issue, we adopted the Chinese tree shrew (*Tupaia belangeri chinensis*), a widely accepted diurnal animal model belonging to the order Scandentia and considered one of the closest extant relatives to primates (30–33). Tree shrews have been used for studying neurophysiology and neuropsychiatric disorders as a day-active model (34–36). They are also most suitable for circuitry studies among different diurnal model animals because they are more accessible and cost-effective, and several viral tools for circuit tracing have been successfully applied to tree shrews. Here, we found that long-term exposure to “early night” LAN impaired mood and cognitive functions in diurnal tree shrews without circadian deterioration and identified a conserved retina-pHb-NAc pathway that mediates the LAN effect on mood but not long-term memory.

## Results

**Tree Shrews Exposed to LAN Exhibit Depressive-Like Behaviors.** We first set out to determine whether prolonged exposure to “early-night” LAN could evoke changes in mood in tree shrews similar to those observed in mice in our previous study (22). Adult male Chinese tree shrews, aged between 6 and 14 mo, were habituated in customized cages equipped with a light-proof sleeping box (nest box) for 3 to 4 wk before undergoing various behavioral assessments (Fig. 1A). Data on locomotion, sucrose preference, circadian rhythm, and cognitive functions were recorded and assessed to ensure that animals had fully adapted to the experimental environment. Animals were then either kept under a regular 8 am to 8 pm photoperiod (control group, Ctrl) or exposed to 2-h blue LAN (~500 lx, between 9 pm and 11 pm), in home-cages with nesting areas illuminated from within, for 3 wk (LAN-exposed group, LAN).

Despite considerable within-group variations, tree shrews subjected to LAN exhibited significant behavioral alterations strongly indicative of depressive-like states. The LAN group of tree shrews had a markedly reduced preference for sucrose (Fig. 1 B–D), while total water consumption was not affected (SI Appendix, Fig. S1 A and B). We also observed a diminished tendency in LAN tree shrews to explore novel items placed inside their home cages, as measured by both numbers of explorations (Fig. 1 E and F) and total exploration time (Fig. 1 G and H), in line with a depressive-like state. During the modeling period, LAN-exposed tree shrews still went in the sleeping box immediately after light-off, and stayed there for the remaining part of the night except for the 2 h when LAN was applied compared to the control group (Fig. 1J). Locomotion of both Ctrl and LAN tree shrews during the daytime was measured as the time and distance moved within 1 h, sampled between ZT4-ZT7 (when tree shrews are most active) before and

after LAN exposure. No significant changes were observed (SI Appendix, Fig. S1 C and D). Together, these data demonstrated that depressive-like behaviors were established in tree shrews by the “early-night” LAN, consistent with our prior findings in mice (22). The briefly applied LAN, although triggered a temporary elevation in locomotion, did not alter the general rhythmicity and structural integrity of the daily activity pattern in diurnal tree shrews (Fig. 1 I and J). Body temperatures monitored using subcutaneous thermo-loggers and locomotion quantified as the active time were also obtained in constant darkness to assess the internal rhythms of the animals. Animals exposed to 3-wk LAN showed statistically indistinguishable rhythms as those kept under 12L:12D conditions, and both were significantly different from the positive control group (15L:9D), suggesting that LAN over 3 wk did not shift the circadian phase of tree shrews (SI Appendix, Fig. S1 E–G).

**LAN Impairs Long-Term Memory in Tree Shrews in the Hole-Board Test.** In addition to mood-related behaviors, we followed through and also examined the learning and memory of three shrews after LAN exposure with the modified hole-board test in our recent study (37). Briefly, 10 holes in a board were marked with either a blue triangle sticker or a yellow square sticker, and only in those marked as yellow squares could tree shrews find yellow mealworms as treats. Animals were trained to retrieve treats from the holes and then tested for how quickly and accurately they were able to perform within a 5-min testing session. Tests were carried out at 1 h, 24 h, and 96 h after a 3-d training period (Fig. 2A). Before LAN exposure, the Ctrl and LAN groups were comparable at all time points, with similar efficiency at accomplishing the task (defined as  $(300 \text{ s} - T_{\text{total}})/300 \text{ s} * 100\%$ ,  $T_{\text{total}}$  refers to the total time used to locate all three targets), and numbers of wrong choices before finding all three treats (Fig. 2 B and C). After 3-wk LAN exposure, the LAN group had similar efficiency and wrong choices to the Ctrl group at 1 h and 24 h (Fig. 2 D and E). Yet the LAN group performed notably worse at 96 h with a lower averaged efficiency, and significantly more wrong choices compared to the Ctrl group (Fig. 2 D and E). These results reflected impaired long-term memory in the LAN group, suggesting that in addition to altered mood, “early-night” LAN also caused deficits in long-term memory in diurnal tree shrews.

**LAN Exposure Does Not Evoke Anxiety-Like Behaviors or Stress Responses.** Tree shrews are well known to be a species relatively vulnerable to stress (38). Chronic stress can cause anxiety-like behaviors and hyperactivity of the hypothalamic–pituitary axis (HPA) in tree shrews, which may manifest as elevated corticosteroid levels and body weight loss (39, 40). To examine whether the depressive-like behaviors we observed in LAN tree shrews were attributed to stress responses, we compared body weight changes and key locomotor parameters related to chronic stress (40), namely the number of times the animal crosses between the nest box and the activity area (crossings), and the number of times the animal jumps in the home cage (jumps). Our data demonstrated that LAN exposure did not cause extra weight loss to the LAN tree shrews in comparison to the control group (SI Appendix, Fig. S2A), neither did LAN induce hypoactivity in LAN tree shrews (SI Appendix, Fig. S2 B and C), arguing against an elevated level of anxiety. Consistently, when we measured the plasma levels of typical stress hormones (SI Appendix, Fig. S2D) and sex hormones (SI Appendix, Fig. S2E) after the LAN exposure, we did not observe any significant endocrine indications for stress in the LAN group, such as elevation of corticosteroids or decreased testosterone (41). We further assessed the correlation between the changes in hormonal levels after LAN exposure and performances

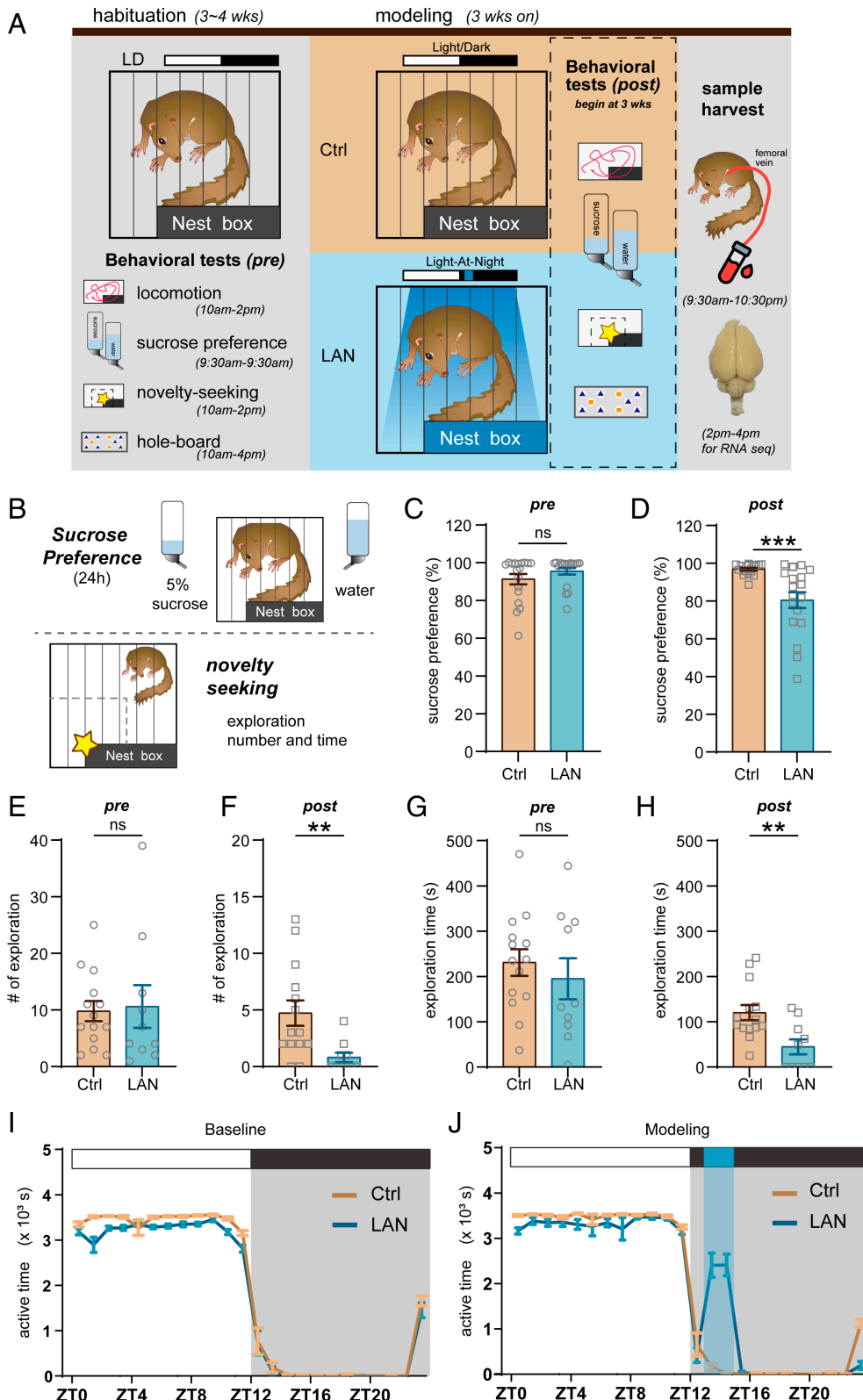


**Fig. 1.** Tree shrews exposed to LAN exhibit depressive-like behaviors. (A) Experimental design for LAN paradigms. Tree shrews were individually housed in cages and allowed to adapt to the new environment and the experimental personnel for a period of 3 to 4 wk. They were maintained under a 12-h light/12-h dark (L/D) cycle from 8 am to 8 pm. All animals underwent behavioral evaluations after they were fully habituated (*pre*). Video recordings of locomotion and novelty seeking were conducted between 10 am and 2 pm. The sucrose preference test was conducted from 9:30 am to 9:30 am the following day. The hole-board test was performed between 10 am and 4 pm. Subsequently, the tree shrews were randomly divided into two groups: the LAN group, exposed to 2 h of blue light (~500 lx) between zeitgeber time (ZT) 13 and ZT 15, and the control (Ctrl) group, which experienced no nighttime illumination. The *post* behavioral tests were performed after the 3-wk modeling period. Finally, all animals were euthanized. Blood and brain samples were collected for further analysis. (B) Schematic diagram of the sucrose preference test and novelty-seeking assay. (C) Sucrose preference was calculated as the proportion of 5% sucrose consumed relative to the total liquid intake (including water and sucrose). Before LAN exposure (*pre*), there was no difference in sucrose preference levels between the Ctrl group (orange) and the LAN group (blue) ( $n = 18$  tree shrews per group;  $P > 0.05$ ; two-tailed unpaired *t* test). (D) After LAN exposure (*post*), the sucrose preference of the LAN group was significantly lower than that of the Ctrl group ( $n = 18$  tree shrews per group;  $P < 0.001$ , two-tailed unpaired *t* test). (E) Before LAN exposure (*pre*), there was no difference in the number of explorations of novel objects between the Ctrl and LAN groups (Ctrl,  $n = 14$ ; LAN,  $n = 10$  tree shrews;  $P > 0.05$ , two-tailed unpaired *t* test). (F) The number of explorations of novel objects in tree shrews following LAN exposure (*post*) was significantly lower relative to the Ctrl group (Ctrl,  $n = 14$ ; LAN,  $n = 10$  tree shrews;  $P < 0.01$ , two-tailed unpaired *t* test). (G and H) Before LAN exposure (*pre*), there was no significant difference in the exploration time for novelty objects between the Ctrl and the LAN group (Ctrl,  $n = 14$ ; LAN,  $n = 10$  tree shrews;  $P > 0.05$ , two-tailed unpaired *t* test). However, after LAN exposure, the LAN group showed a significantly reduced exploration time compared to the Ctrl group (Ctrl,  $n = 14$ ; LAN,  $n = 10$  tree shrews;  $P < 0.01$ , two-tailed unpaired *t* test). (I and J) The hourly activity level of tree shrews before the experiment (I) and under LAN conditions (J) ( $n = 3$  tree shrews per group; each animal was recorded and measured over three consecutive days). The x-axis represents the ZT time points, with shaded areas indicating dark periods and blue areas indicating light at night. The Ctrl group is represented by the orange line, while the LAN group is represented by the blue line. Values are presented as mean  $\pm$  SEM. ns, not significant; \*\* $P < 0.01$ ; \*\*\* $P < 0.001$ .

in behavioral assays in a subgroup of randomly selected LAN tree shrews. Cortisol and testosterone were used as representative hormones, and correlative analysis revealed that none was correlated with sucrose preference (*SI Appendix*, Fig. S2F), suggesting that decreased sucrose preference was unlikely to be a result of elevated HPA activity. Similarly, changes in cortisol or

testosterone levels were not correlated with the number of wrong choices in the hole-board test (*SI Appendix*, Fig. S2G). Collectively, these data showed that LAN-exposed tree shrews did not exhibit typical behavioral or endocrine hallmarks of stress responses. Thus, the depressive-like phenotype we observed was likely to be a direct result of the activation of visual circuits.

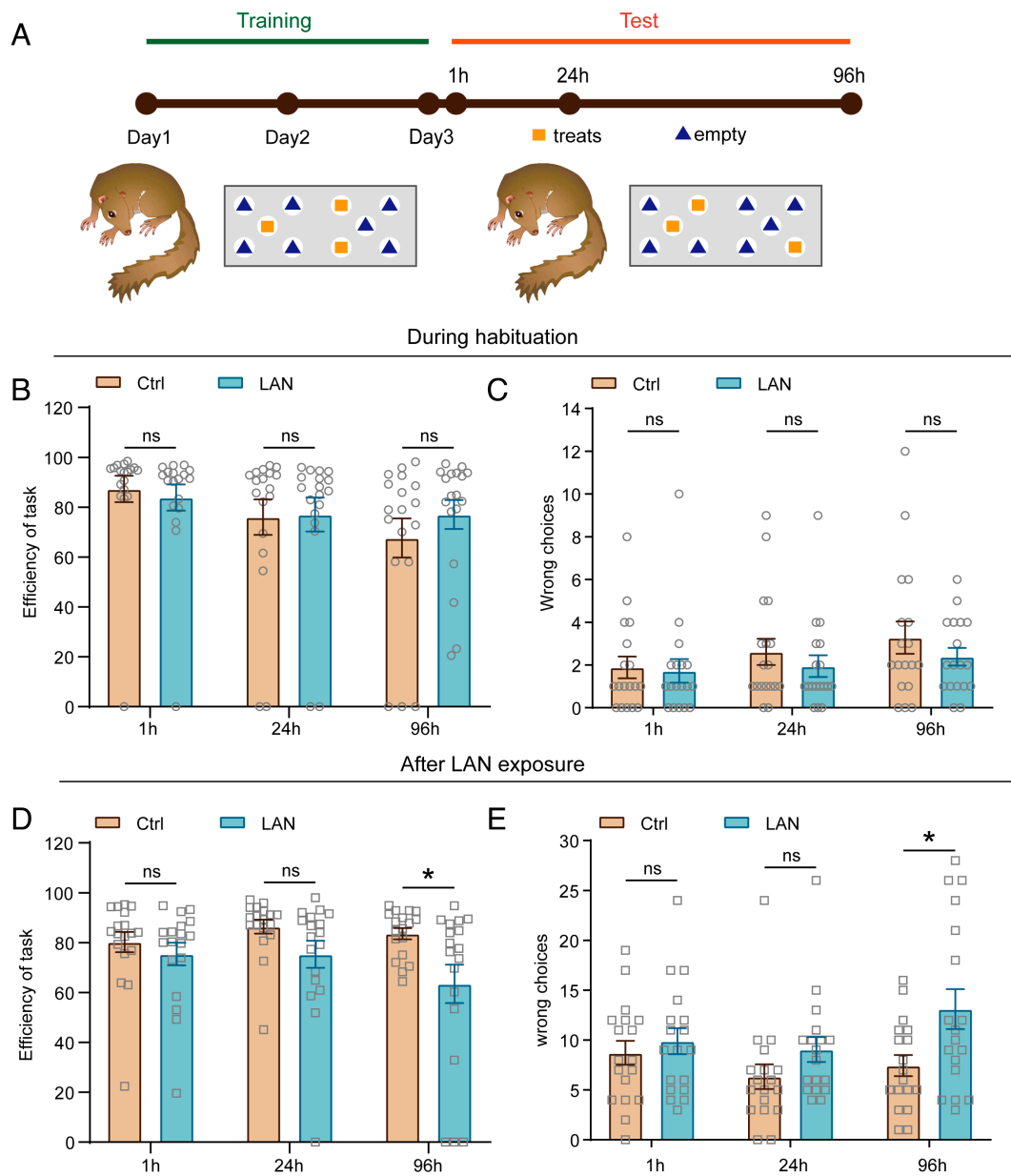


**Fig. 2.** LAN impairs long-term memory in tree shrews in the hole-board test. (A) Experimental design for hole-board test. (B and C) Performance of tree shrews during the habituation stage. Wrong choices (touching nontarget holes before locating all three target holes) were counted. Efficiency was quantified as the percentage of remaining time after the tree shrew completed the task in a total time of 300 s. Before LAN exposure, there were no differences in the efficiency of task completion (B) and the wrong choices (C) during the task between the Ctrl group (orange) and the LAN group (blue) of tree shrews at 1 h, 24 h and 96 h. (D and E) Performance of tree shrews after LAN treatment for 3 wk. There were no significant changes of efficiency and wrong choices at the 1 h and 24 h (D and E), but a significant difference in efficiency was observed between the LAN group and the Ctrl group at 96 h (D), and the number of wrong choices of the LAN group was significantly lower at 96 h relative to the Ctrl group (E). Each group has 18 tree shrews. Values are presented as mean  $\pm$  SEM. ns, not significant; \* $p$  < 0.05; Two-way ANOVA, Tukey's post hoc test.

**Retinal Ganglion Cells (RGCs) Project to the Mood-Related pHb in Tree Shrews.** To establish the precise structure of the visual circuit that may underlie the LAN effects in the diurnal tree shrew, we employed classic techniques for circuitry studies in rodents. We examined whether retinal projections to the pHb, an important node recently revealed (22), were conserved in tree shrews. We first challenged tree shrews with a brief 10-min blue illumination at ZT13 under complete darkness to mimic the LAN stimulation, and then evaluated the c-Fos protein abundance around the pHb in naïve (Ctrl) and light-challenged (Light) tree shrews (Fig. 3A). Quantifications revealed a significant increase of c-Fos<sup>+</sup> cells induced by the brief LAN (Fig. 3B), suggesting direct or indirect functional connectivity of photic information from the retina to the pHb area.

To further determine whether there exist direct retinal inputs to the pHb in tree shrews, we conducted tracing experiments using either tracing dye CTB-555 (Cholera toxin subunit B conjugated to a fluorescent probe) or tracing viruses, following the procedure in our previous study (22). As expected, intravitreally delivered CTB-555 (Fig. 3C) anterogradely labeled axonal tracts of the optic nerve (Fig. 3D) and axonal terminals of the optic nerve in the pHb (Fig. 3E). Next, we performed trans-synaptic anterograde tracing using AAV1-Cre, a well-established viral tool producing Cre recombinase that can be transported through monosynaptic connections to post-synaptic neurons (Fig. 3F). AAV1-Cre was ocularly injected, and infected RGCs including their axons were labeled red due to the expression of a red fluorescent protein

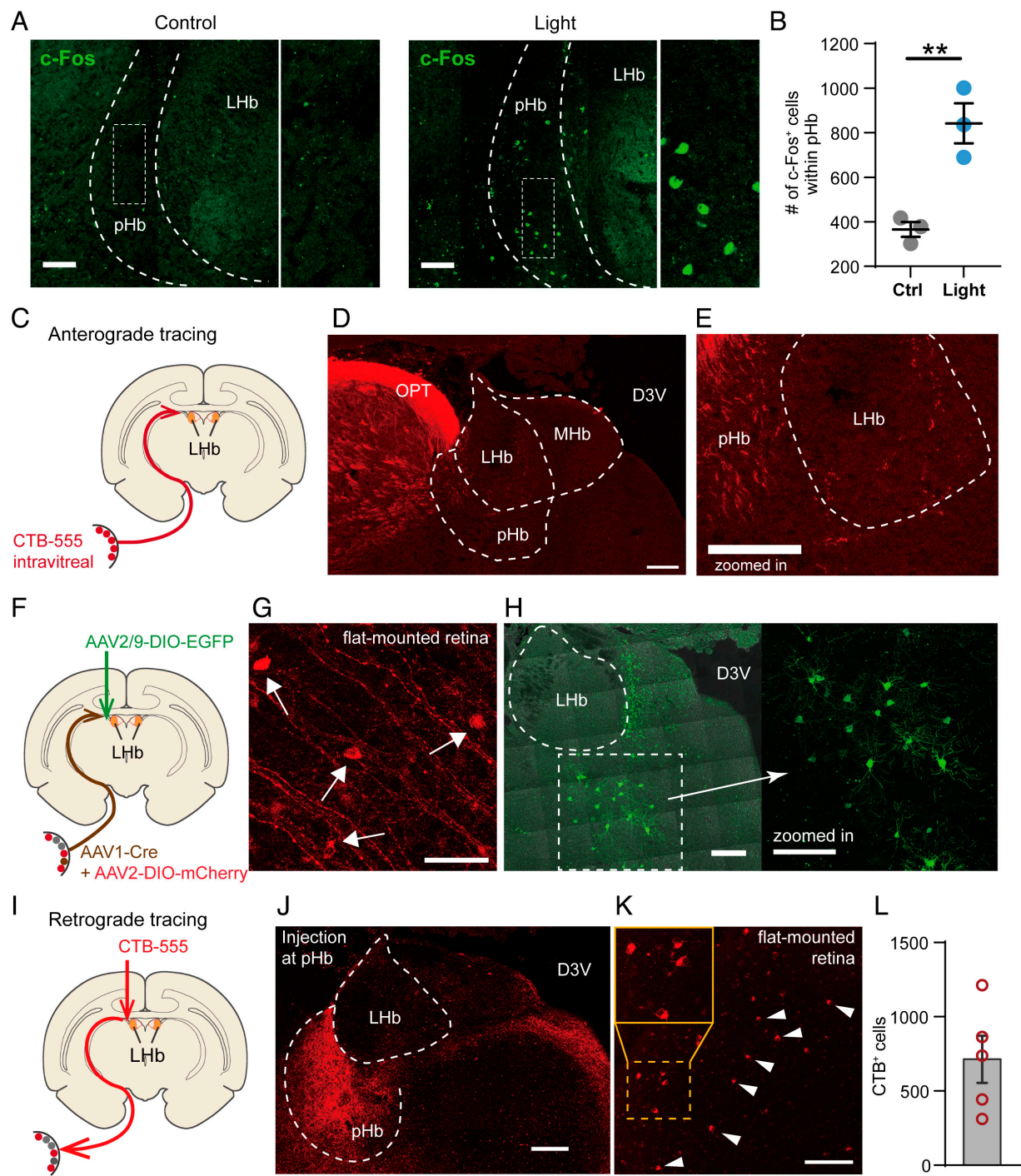


**Fig. 3.** Retinal projections to the pHB in tree shrews. (A) Immunohistochemical staining of c-Fos in the pHB brain region was performed on tree shrews exposed to light (Light) and without light (Control) during the night. (Scale bar, 100 μm.) (B) The number of cells positive for c-Fos immunoreactivity within the pHB area was quantified for each individual tree shrew in control group (Ctrl) and light exposed group (Light). A significant increase in the number of c-Fos<sup>+</sup> cells was observed in the Light group compared to the Ctrl group ( $n = 3$  tree shrews;  $P < 0.01$ , two-tailed unpaired  $t$  test). (C) Schematic diagram depicting anterograde tracing with intraventricularly injected cholera toxin subunit B (CTB-555) tracers. (D and E) Anterograde tracing with CTB showing axonal terminals of the RGCs within the pHB. The tracing experiment was independently repeated at least three times with similar results. The lined areas pHB, perihabenular nucleus. LHb, lateral habenular nucleus; OPT, optic tract; MHb, medial habenular nucleus; D3V, dorsal 3rd ventricle. (Scale bar, 200 μm.) (F) Schematic diagram of anterograde trans-synaptic tracing from the retina to the pHB. Intraventricular AAV1-Cre was combined with Cre-dependent EGFP delivered into the pHB to label pHB neurons that receive direct synaptic inputs from the RGCs. (G) Starter RGCs (white arrows) on a flat-mounted retina labeled with Cre-dependent mCherry (AAV2/2-DIO-mCherry). (Scale bar, 50 μm.) (H) GFP-expressing RGC-innervated neurons (close-up view shown on the Right) in the pHB. (Scale bar, 200 μm.) The tracing experiment was independently repeated two times with similar results. (I) Schematic diagram of retrograde tracing from the pHB with CTB-555 injected into the pHB. (J) Red fluorescence at the injection sites. (Scale bar, 200 μm.) (K) Retrogradely labeled pHB-projecting RGCs (white arrowheads) on a flat-mounted retina. (Scale bar, 100 μm.) Close-up view of the representative section outlined by yellow dashed lines was shown on the *Upper Left*. (L) Quantification of the labeled retinal RGCs in tree shrews used for (I) ( $n = 5$  retina from four tree shrews). Cells were manually counted by the experimenter. Values are presented as mean ± SEM. \*\* $P < 0.01$ .

mCherry under the control of Cre (Fig. 3G). Combined with AAV2/9-DIO-EGFP (expressing the green fluorescent protein in a cre-recombinase-dependent manner) stereotactically delivered to

the pHB, we were able to identify pHB neurons that receive monosynaptic inputs from the retina (Fig. 3H). The number of RGCs that feed to the pHB was estimated, with retrograde tracing from

the pHb using CTB-555 (Fig. 3 *I–L*), to be around 700 to 800 cells per retina.

**The pHb Is Required for the LAN Effect on Mood but Not Long-Term Memory.** Based on the above viral-tracing results, the retina-pHb-NAc pathway we identified in mice (22) is likely to be conserved in tree shrews, it is thus essential to establish whether this pathway contributes to the depressive-like behaviors induced

by “early-night” LAN similar to what was found in mice. To this end, we conducted excitotoxic lesion of the pHb (*Materials and Methods*) and validated the lesions with NeuN immunostaining as a marker for viable neurons (Fig. 4*A*). The post-hoc examination showed a dramatic reduction in the numbers of neurons in the pHb but not in the nearby lateral habenula (LHb) area (Fig. 4*B*), nor in the PF (dorsal nucleus of the pulvinar, lateral to the pHb), PD (dorsal nucleus of the pulvinar, ventral to the pHb), and PVP

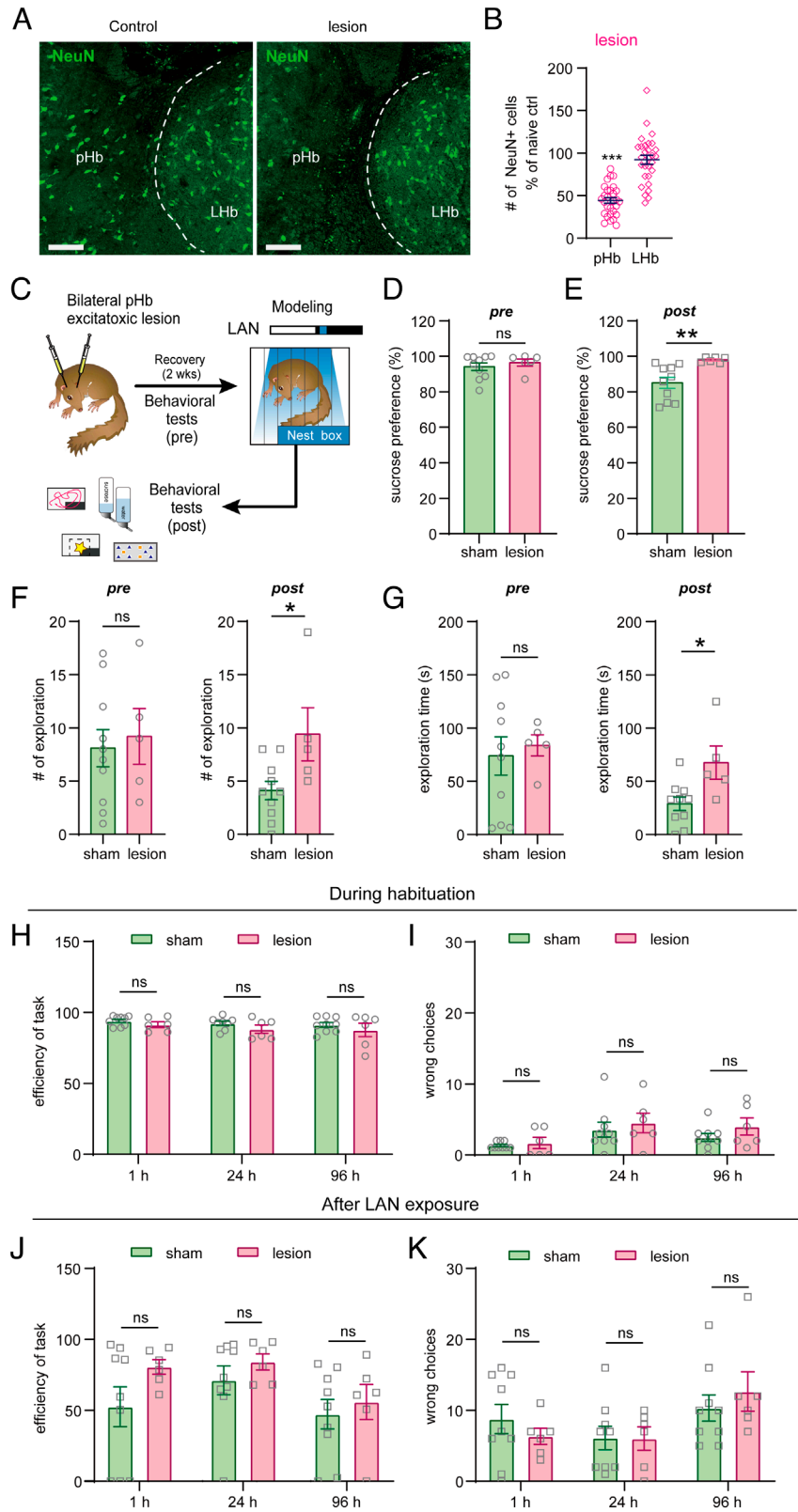


**Fig. 4.** LAN effect mood requires the pHb in tree shrews. (A) NeuN staining in naïve (Control) and excitotoxicity lesioned (lesion) tree shrews, with green fluorescence indicating viable neurons (positive for NeuN). The LHb was distinguished from pHb by dashed lines. (Scale bar, 100  $\mu$ m.) (B) Quantification of NeuN-positive cells in the pHb and LHb regions of lesioned tree shrews relative to the averaged cell count in the respective areas in naïve animals. In lesioned animals there was a significant decrease in NeuN-positive cells in the pHb area but not the LHb area (lesion group,  $n = 29$  tree shrews, \*\*\*: significantly different from the Control group,  $P < 0.001$ , two-tailed unpaired  $t$  test). (C) Experimental design for assessment of LAN effect on tree shrews with pHb-excitotoxic lesion. (D) Before LAN exposure (pre), there was no difference in sucrose preference levels between the sham group (green) and the lesion group (pink) (sham,  $n = 10$ , lesion,  $n = 6$  tree shrews;  $P > 0.05$ ; two-tailed unpaired  $t$  test). (E) After LAN exposure (post), the sucrose preference of the sham group was significantly lower than that of the lesion group (sham,  $n = 10$ , lesion,  $n = 6$  tree shrews;  $P < 0.01$ ; two-tailed unpaired  $t$  test). (F) The number of explorations of novel objects was not significantly different between the sham group and the lesion group before LAN (pre) (sham,  $n = 10$ , lesion,  $n = 5$  tree shrews;  $P > 0.05$ ; two-tailed unpaired  $t$  test). However, after LAN exposure (post), the sham group exhibited a significantly lower number of explorations compared to the lesion group (sham,  $n = 10$ , lesion,  $n = 5$  tree shrews;  $P < 0.05$ ; two-tailed unpaired  $t$  test). (G) Before LAN (pre), there was no difference in the number of explorations of a new object between the sham group and the lesion group (sham,  $n = 10$ , lesion,  $n = 5$  tree shrews;  $P > 0.05$ ; two-tailed unpaired  $t$  test). However, the sham group tree shrews following LAN (post) exhibited a significant decrease relative to the lesion group (sham,  $n = 10$ , lesion,  $n = 5$  tree shrews;  $P < 0.05$ ; two-tailed unpaired  $t$  test). (H and I) In the hole-board test, there were no significant difference in the efficiency (H) and the number of wrong choices (I) between two groups at 1 h, 24 h and 96 h (sham,  $n = 9$ , lesion,  $n = 6$  tree shrews;  $P > 0.05$ ; two-way ANOVA, Tukey's post hoc test.). (J and K) After LAN treatment for 3 wk, there was no significant difference in the efficiency and the number of wrong choices between sham and lesion groups at 1 h, 24 h, and 96 h (sham,  $n = 9$ , lesion,  $n = 6$  tree shrews;  $P > 0.05$ ; two-way ANOVA, Tukey's post hoc test.). Values are presented as mean  $\pm$  SEM. ns, not significant; \* $P < 0.05$ ; \*\* $P < 0.01$ ; \*\*\* $P < 0.001$ .

(paraventricular thalamic nucleus, posterior part, surrounding the 3rd ventricle) regions (*SI Appendix*, Fig. S3B), confirming an effective local lesion in the NMDA-treated group (Fig. 4B). The parallel-treated sham group with PBS injections showed no detectable sign of cell loss (*SI Appendix*, Fig. S3A). We then subjected both sham-operated (sham) and the lesioned (lesion) tree shrews to the same “early-night” LAN paradigm (Fig. 4C). Interestingly, the depression-inducing effect of LAN was mitigated in the lesioned but not sham animals, as evidenced by a higher sucrose preference in the lesioned animals compared to the sham controls (Fig. 4D and E and *SI Appendix*, Fig. S3C). In novelty-seeking assay, reduced exploratory behaviors were observed after LAN exposure in the sham animals compared to the lesioned animals (Fig. 4F and G). In another set of experiments in which key behavioral parameters of NMDA lesioned tree shrews were compared before and after LAN treatment in a self-control manner, we found no decrease of sucrose preference or reduction in novelty seeking (*SI Appendix*, Fig. S4A and B), supporting the notion that functional ablation of the pHb area endowed animals resistance to the LAN-induced negative mood. As with naïve animals, LAN also had a minimum effect on the general rhythmicity of the animal circadian rhythm except for a temporary elevation in activity level within the 2-h blue light window (*SI Appendix*, Fig. S4C).

Surprisingly, the LAN-induced impairment of long-term memory was seemingly insensitive to the pHb lesion. Sham animals and lesioned animals were not statistically different in both pre and post windows in terms of efficiency and number of wrong choices (Fig. 4H–K). These data may suggest that LAN affects mood and cognitive functions such as learning and memory via separate pathways, with the latter not involving a functional pHb. Finally, neither sham nor lesioned tree shrews exhibited reductions in body weight (*SI Appendix*, Fig. S3D) or deficits in locomotion (*SI Appendix*, Fig. S3E), just as previously observed with naïve tree shrews. Collectively, our findings point to the pHb as a key region in the detrimental effects of LAN on mood, but not long-term memory.

### The pHb Provides Inputs to the Mood Center NAc in the Tree Shrew

**Brain.** In mice, pHb receives inputs from the retina carrying photic information and in turn conveys these cues to the NAc, a mood regulatory center, to induce depressive-like behaviors (22). Thus, we examined whether such connections are evolutionarily conserved in tree shrews. We injected the tracing dye CTB-555 into the NAc (Fig. 5A and B) and found clusters of clearly labeled cells in the pHb (Fig. 5C). Those retrogradely labeled NAc-projecting neurons were distributed near the margins of the habenular nucleus (LHB) along the rostral-caudal axis (Fig. 5D), coinciding with what was observed in mice (22). Anterograde tracing using viral tools from the pHb with AAV1-Cre injected into the pHb and AAV2/9-DIO-EGFP delivered to the NAc revealed post-synaptic NAc neurons (Fig. 5E and F), providing evidence that the pHb innervates the NAc in the diurnal tree shrew. Finally, we labeled pHb neurons that receive monosynaptic inputs from the retina using AAV1-cre combined with Cre-dependent EGFP (Fig. 5G; same procedure as in Fig. 3F), then examined the NAc for axonal terminals of the anterogradely labeled pHb neurons. We found clear fluorescent signals in the NAc area (Fig. 5G and H), suggesting that pHb neurons receiving ganglion cell input indeed continue to project to the NAc.

**Transcriptomic Profiling Revealed Changes in Depression-Related Genes and Pathways within the NAc Following LAN Exposure.** Brain samples containing the NAc area from control (Ctrl) and LAN-exposed (LAN) tree shrews (2 from each group) were collected for RNA-sequencing analysis. Data acquired from all four samples were first normalized following standard

routine and then subjected to quality control examination (42). The density plot and violin plot of gene expression distribution demonstrated decent and comparable qualities among samples (Fig. 6A and B), suggesting a high level of consistency regarding the sample quality. Detailed analysis revealed 343 significantly up-regulated or down-regulated genes in LAN exposed animals compared to control animals, including several key genes in the regulation of perineuronal net (PNN) (*HAPLN4* and *NCAN*), synaptic transmission (*HTR1A*, *HTR2A*, and *CRHRI*), and ion channel activity (*CAMK2D*) (Fig. 6C and D and *SI Appendix*, Fig. S6). The GSEA (gene-set enrichment analysis) also revealed a significant change in the calcium signaling in the depression pathway (Fig. 6E). Altogether, these findings suggest plastic changes at the transcript level taking place within the NAc following long-term exposure to LAN.

### Discussion

Light, as a universal factor of the external environment, substantially impacts many physiological processes that at the same time influence each other (43). It is thus often not readily obvious whether a certain effect of light is conveyed via direct or indirect routes. As for light in mood regulation, it has now become clear that light could affect mood via both direct and indirect pathways, thanks to several delicate studies looking into the underlying neuronal circuitry mechanisms (11, 22, 44, 45). Our current study with the use of a diurnal primate-like model animal, tree shrew, identified a direct visual pathway likely responsible for the LAN-induced depressive-like behaviors in diurnal animals. These findings, combined with our previous work in mice (22), provide a more comprehensive understanding of light-induced mood modulation in diurnal and nocturnal animals.

In our prior mouse study, we first identified the retina-pHb-NAc pathway responsible for the direct effect of LAN in inducing depressive-like behaviors, and showed that photophobia-related components were insufficient to cause mood changes in our LAN paradigm (22). In the current study of the diurnal tree shrew, LAN exposure does not provoke photophobia but could lead to other by-products such as disrupted sleep and long-term stress that are worth considering when discussing mood regulation (29, 46). Long-term exposure to various forms of LAN could lead to sleep deprivation and circadian deterioration, which are known to contribute to negative mood changes (13, 18). To address this possibility, we conducted experiments with the pHb-lesioned tree shrews. Lesioned tree shrews experienced brief disturbances of early night sleep similar to naïve tree shrews when exposed to LAN, yet did not exhibit signs of depression as indicated by unchanged sucrose preference and exploration of novel items. These findings suggest that the mild sleep perturbation observed in tree shrews when exposed to LAN was not adequate to induce depressive behavioral changes, and disruption of pHb function is sufficient to confer protection against LAN-induced negative mood. Altogether, findings from both nocturnal and diurnal animals may point to a common principle in mood regulation by light. Light is merely a neutral representation of the solar circle, regardless of the specific chronotype of an animal. This notion is supported by the fact that light modulates the SCN in a fairly similar manner in both chronotypes (26). Therefore, it is not a surprise that we have observed that 3-wk LAN exposure induced similar depressive-like behaviors in both diurnal and nocturnal animals, likely involving conserved direct neural pathways. It should also be noted that, though in the present study 3-wk LAN did not shift the circadian phase, it remains a possibility that over a longer period of exposure, internal circadian rhythms may be affected by repeated appearance of 2 h bright light during

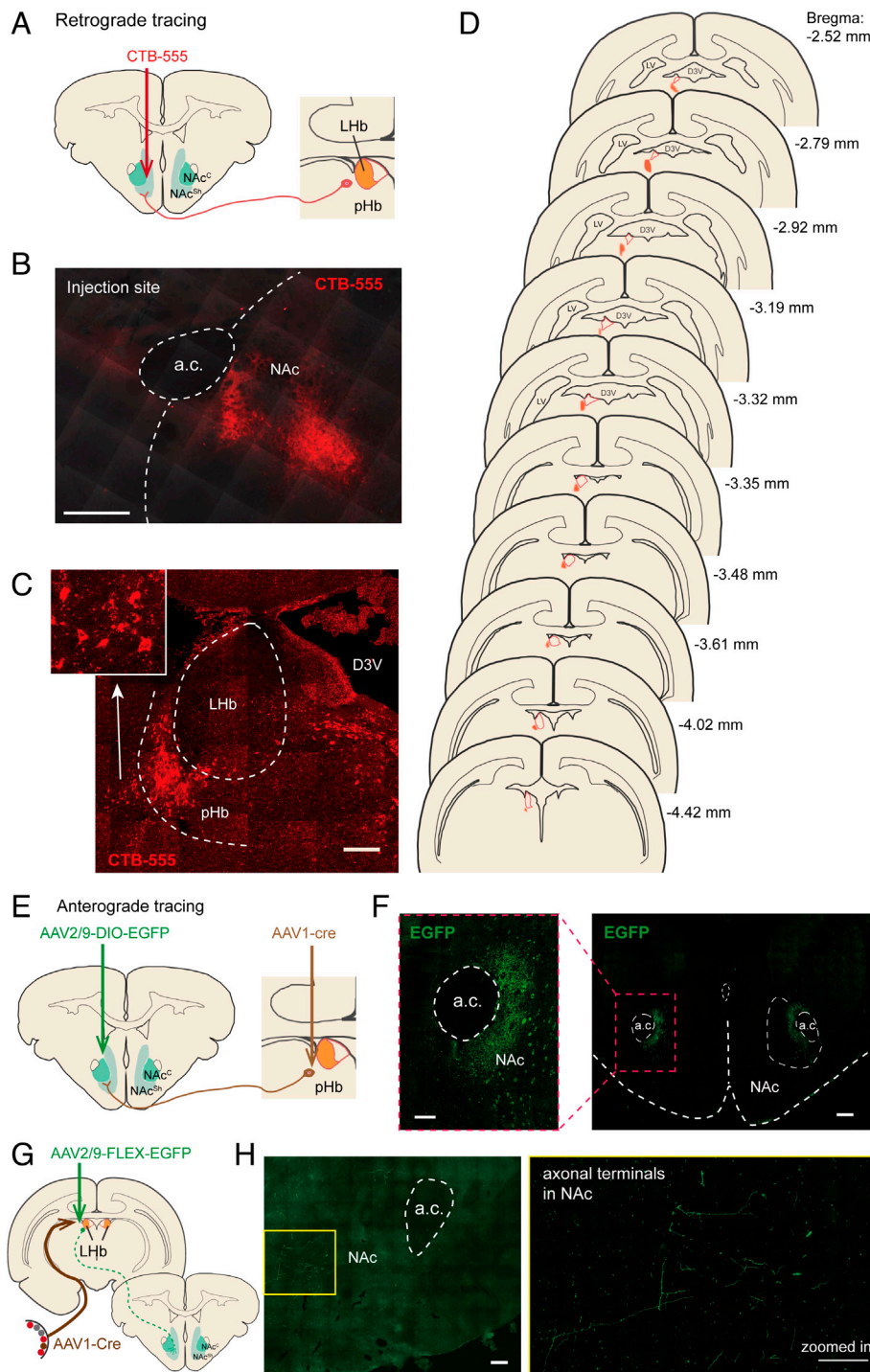


**Fig. 5.** Characterization of pHB inputs to the NAc in the tree shrew brain. (A) Schematic diagram of retrograde tracing from NAc. CTB-555 was injected into the NAc. Experiments were independently repeated five times with similar results. (B) Red fluorescence from CTB-555 at the injection site in NAc. (C) Retrogradely labeled NAc-projecting pHB neurons (close-up view shown in *Inset*). (D) Line drawings showing the distribution of retrogradely labeled NAc-projecting neurons near the LHB (red outline) on serial brain slices. Numbers indicate the distance (mm) away from bregma. (E) Schematic diagram of anterograde trans-synaptic tracing. Anterograde tracing AAV1-Cre was combined with Cre-inducible EGFP delivered into the NAc to label NAc neurons that receive direct synaptic inputs from the pHB neurons. (F) GFP-expressing pHB-innervated neurons in the NAc (close-up view of the representative section outlined in red dashed lines is shown to the *Left*, a.c.: anterior commissure). (Scale bar, 500  $\mu$ m.) The tracing experiment was independently repeated at least three times with similar results. (G) Schematic diagram of anterograde trans-synaptic tracing. (H) Terminal field of RGC-innervated pHB neurons in the NAc and close-up view. (Scale bar, 500  $\mu$ m.)

the night, even eventually incorporating LAN into an extended day. In that case, LAN may affect physiology via direct and indirect pathways at the same time, which requires further investigations.

Interestingly, the pHB, a recently defined nucleus surrounding the habenula nucleus in the thalamus (11), appeared differentially involved in the regulation of mood versus long-term memory by light. We found that tree shrews with excitotoxic lesions of the pHB did not exhibit depressive behaviors after 3 wk of LAN exposure, yet were still impaired in long-term memory. This observation, consistent with prior findings in rodents (11), suggests that LAN exposure in tree shrews affects mood and memory through divergent pathways, with the pHB being a key region in the former

but not the latter. To pursue the precise mechanism underlying the memory deficits induced by long-term LAN exposure in tree shrews is beyond the focus of the current study, however, whether it was mediated by another direct neural pathway or a secondary effect following disturbed sleep deserves further studies.

The NAc, downstream of the pHB as revealed by our circuit tracing experiments in this study, is a key component in reward and motivation, and the central reward pathway has been strongly indicated in various mood disorders including depression (47). Tree shrews exhibited behavioral hallmarks of depression such as anhedonia and decreased motives, which may be consequences of a dysregulated NAc. A recent study showed that NAc-linked executive

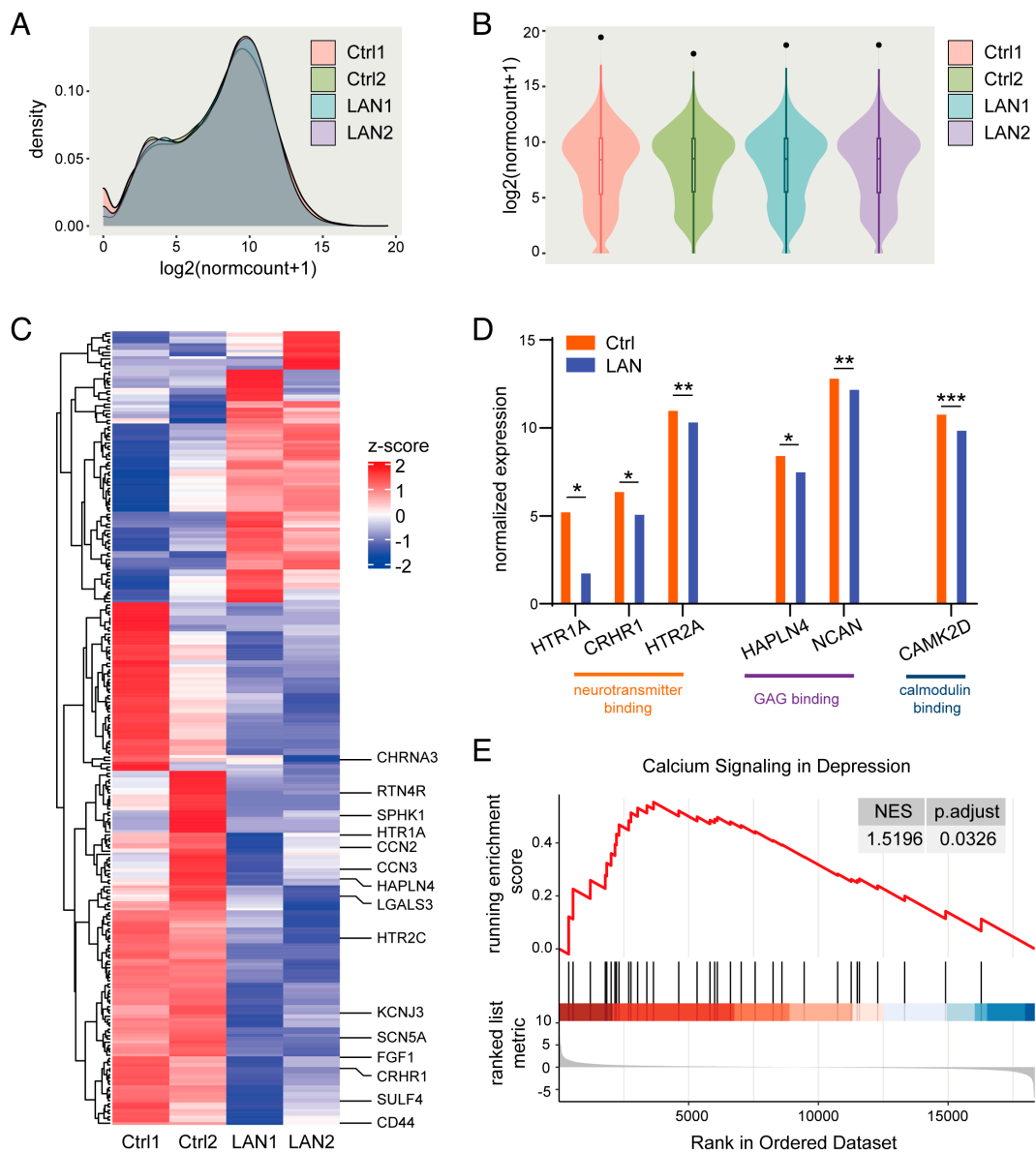


**Fig. 6.** Transcriptomic analysis reveals changes in depression-related genes and pathways within the NAc following LAN exposure. (A) Normalized expression density distribution plot. The control group (Ctrl) consisted of two animals, designated Ctrl1 and Ctrl2. LAN1 and LAN2 comprise the LAN group. These tree shrews were killed for brain tissue collections after having finished the related behavioral tests in Fig. 2. (B) Violin plots showing normalized counts from DESeq2 for all samples. (C) Heatmap of differentially expressed genes associated with depression in NAc between the Ctrl and LAN groups, the color bar represents the z-score of the gene expression. (D) Selected depression-related genes that are downregulated in the NAc samples harvested from LAN-treated animals relative to the control tree shrews. (E) Gene set enrichment analysis diagram of changes in depression signaling pathway between the two groups.

control networks mediate reversal learning in tree shrews (48). Interestingly, we found significant transcriptional changes in NAc tissues from LAN-exposed tree shrews that may be associated with depressive behaviors, including multiple genes involved in the regulation of PNN, synaptic transmission, and ion channel activity. PNN is a specialized extracellular matrix structure, often enwrapping parvalbumin-positive (PV<sup>+</sup>) neurons (49). Members of the chondroitin sulfate proteoglycan (CSPGs) family, including aggrecans, versican, brevican, and neurocan (NCAN), are major constituents of all PNNs, with hyaluronan forming the backbone (50). PNN plays a critical role in neuronal plasticity and contributes to affective states (51). Changes in PNN protein in the NAc affect motivated behaviors (52). In rats with chronic-stress-induced depression, PNN density in mood centers is significantly reduced, which could be reversed by antidepressive drugs (53). We found moderate yet significant changes of NCAN and HAPLN4 mRNA expression levels following LAN exposure. NCAN is a key component of the PNN

and HAPLN4 mediates the binding of CSPGs to the hyaluronan backbone. Downregulated expression of those critical genes might result in reduced density of the PNN and dysregulated excitatory versus inhibitory signals in the NAc. We also found a marked reduction in the expression level of serotonin receptors HTR1A and HTR2A, both of which are closely associated with depressive symptoms (54–56). Pathway enrichment analysis of differentially expressed genes in LAN exposed animals relative to control ones further revealed a moderate yet significant change in calcium-signaling in depression. The changes in depression-associated genes and pathways in the NAc following LAN exposure are likely relevant to the LAN-induced depressive behaviors in tree shrews.

Research on light modulation of mood is not only to fulfill our endless curiosity on how our nervous system responds to the changing outside world but also to meet the increasing demand of fighting the detrimental impact of light pollution. Hence, animal models that are more similar to humans in terms of physiological

responses to light are indeed a necessity. Tree shrews are day-active, primate-like model animals with fully sequenced genome and a standard full brain atlas (42, 57). They are also relatively more cost-effective compared to primates in terms of reproduction and maintenance. Efforts have been made to optimize viral tools for circuit tracing and functional manipulations in tree shrews, making it an accessible and suitable diurnal model for circuitry study. On the downside, tree shrews are also known to be a stress-prone species (58), and exhibit much higher variability among individuals than other common lab animals such as rats and mice. In our experience, different batches of tree shrews tend to show greater variabilities in behavioral assays and may vary in their responses to changing environmental factors such as season, weather, or other possible factors, which hinders long-term neurophysiological studies. Therefore, establishing an inbred line of tree shrews will greatly facilitate future research using this diurnal model species.

In short, we found LAN negatively affects mood in tree shrews via a visual pathway related to the pHb. Our findings as an attempt to decipher a functional pathway in tree shrews may pave the way to more mechanistic research in diurnal animals and generate valuable datasets for translational work aiming to prevent or treat mood disorders associated with excessive LAN.

## Materials and Methods

**Animals.** The Chinese tree shrews (*Tupaia belangeri chinensis*) were obtained from the Kunming Institute of Zoology, Chinese Academy of Sciences. Animal housing and all experimental procedures were in compliance with the guidelines of the Institutional Animal Care and Use Committee of the Kunming Institute of Zoology, Chinese Academy of Sciences.

Adult male tree shrews (6 to 14 mo old; body weight 100 to 160 g) were used for all experiments. Animals were individually housed in controlled conditions within stainless steel cages (size 600 × 600 × 800 mm, w × d × h). Nest boxes (size 160 × 350 × 200 mm, w × d × h) were attached to the front of the cages, providing sleeping quarters for the animals. Water and diet were available ad libitum. White and blue light panels were installed atop the cages, and blue light panels were also installed in the nest boxes. Tree shrews were allowed to adapt to the new environment and experimenters for at least 3 wk. They were maintained under an 8:00 to 20:00 12 h:12 h light/dark cycle (250 to 300 lx white ambient illumination) except for during LAN exposure (450 to 500 lx blue illumination between 21:00 and 23:00). The spectra of both "white" and "blue" light stimuli were measured in nanometers (380 nm to 780 nm) using a radiometer (SRC-200S, Everfine Photo-e-Info CO., Ltd, China) and provided in *SI Appendix, Fig. S5*. Video cameras were installed above the cages to record the diurnal and nocturnal activity states as well as fine movements of tree shrews.

**Intraocular Injection.** The pupil-dilating eye drops [1% w/v atropine (Aladdin A109524) and 5% w/v phenylephrine hydrochloride (Aladdin P106007)] were administered to induce pupil dilation. After approximately 5 min or until full dilation of the pupils, tree shrews were anesthetized with ketamine (i.m. 50 mg/kg) and sodium pentobarbital (i.m. 60 mg/kg). The pupil was penetrated with the tip of a 26-gauge needle under the stereoscope to release ocular pressure. Two small punctures were made on both the nasal and temporal sides of the tree shrew cornea. Excess aqueous humor was absorbed using a cotton swab. To minimize the damage to vision, the needle tip was carefully operated to avoid touching the retina and lens. Using a Hamilton syringe (Model 65 RN SYR with a customized 33-gauge needle), a total of 5  $\mu$ L of virus or tracing dye was injected into the space between the lens and the retina through the two punctures, ensuring even distribution. Following surgery, eye gel (5% sodium carboxymethyl cellulose) was used to prevent eyes from drying, and tree shrews were allowed to recover from anesthesia on a heating mat before being returned to their home cages.

**Stereotaxic Injection.** Adult tree shrew was anesthetized with ketamine (i.m. 50 mg/kg) and sodium pentobarbital (i.m. 60 mg/kg). Subsequently, the tree shrew was positioned on a stereotaxic apparatus (Shenzhen RWD Life Science), and erythromycin ointment (Guangdong Hengjian Pharmaceutical Co., Ltd) was applied to prevent corneal dryness. The scalp was shaved and cleaned, followed by making a

linear incision on the skin to expose the skull, which was subsequently cleaned with a cotton swab dipped in phosphate-buffered saline (PBS). The skull above the target area was drilled open for stereotaxic injection using a micropump (Shenzhen RWD Life Science KDS LEGATO 130). Either 400 nL of virus or 250 nL of dye was delivered into the brain at a rate of 50 nL per min, followed by an additional 15-min delay to prevent leakage and ensure a localized lesion. For excitotoxic lesion, 210 nL of NMDA solution (50 mM) was injected at the rate of 30 nL per min with an additional 15-min delay. The specific volumes of injected dyes/viruses were either adopted from published studies or estimated from rodent experiments (59–61). These tree shrews were killed for the injection area verification after having finished the related behavioral tests. Brain regions were identified and located using the published atlas of *Tupaia* (57). The coordinates, defined as dorsal–ventral (DV) from the brain surface, anterior–posterior (AP) from bregma and medial–lateral (ML) from the midline, were as follows: NAc (AP, +2.47 mm from bregma; ML,  $\pm 1.74$  mm; DV,  $-7.17$  mm); pHb (AP,  $-3.9$  mm from bregma; ML,  $\pm 1.07$  mm; DV,  $-5.70$  mm). Pilot experiments were conducted using the same coordinates following the same procedure to inject Nissl stain to label the injection site, and the location was compared with the brain atlas to ensure the coordinates of target brain regions were precise. After completion of the injection, the injection pipette was slowly withdrawn and the scalp was closed. Following surgery, erythromycin ointment was applied to the wound to prevent infection, and tree shrews were allowed to recover from anesthesia on a heating mat before being returned to their home cages. Injections were later examined by the experimenters after samples were collected. Fluorescence from dyes or viruses, injection traces, and localized tissue damages were all used to assess the location and extent of the injections.

**Immunohistochemistry.** Tree shrew was anesthetized following the above procedure, then intracardially perfused with PBS and subsequently with 4% paraformaldehyde (PFA, w/v in PBS). The brain was then removed, post-fixed in 4% PFA at 4 °C for 72 h, and later subjected to dehydration in 30% (w/v) sucrose solution. Coronal sections were prepared at a thickness of 50  $\mu$ m using a Cryostat microtome (Leica CM3050S). After air-drying at room temperature, antigen retrieval was performed by heating the tissue sections in sodium citrate solution (Shanghai Sangon Biotech Co., Ltd. A610035) at 92 °C for 1 h. Subsequently, the brain slices were blocked with blocking solution (PBS containing 5% BSA, 5% goat serum, and 0.5% Triton X-100) for 1.5 h at room temperature. The samples were then incubated overnight at 4 °C with the appropriate primary antibody. Following incubation with the indicated primary antibody, the sections were rinsed with PBS (3 × 5 min) and exposed to the respective secondary antibodies for 2 h at room temperature. Antibody details are provided in the *SI Appendix, Supplement Materials and Methods*.

Finally, the sections were examined and imaged under a ZEISS two-photon microscope (LSM980+, ZEISS). Images were analyzed and quantified by researchers blind to the experiment groups using ImageJ software. Cells in different brain regions were counted by the same experienced researcher using the same criteria.

**Randomization and Blinding.** For behavioral experiments, tree shrews were randomly assigned to various treatment groups. The data collectors were not blind to the group assignment of the object as they needed to record the sample or animal identifier. However, data analysis was performed either using automated software with consistent parameters or by investigators who were blind to the experimental conditions.

**Sucrose Preference Test.** We followed the previously reported procedure to test the tree shrew's sucrose preference (62). In brief, tree shrews were acclimatized to two bottles for 24 h, with one containing water and the other containing a 2% sucrose solution. Tree shrews were then subjected to water deprivation for 24 h, followed by the 24-h testing period (starting from 9:30 am), during which the tree shrews were provided with one bottle of 5% sucrose and one bottle of water. The positions of the two bottles were alternated at 2 h and 6 h. Sucrose preference was calculated as the proportion of 5% sucrose in the total amount of liquid consumed (water and sucrose). The average data obtained at 3 and 4 wk of LAN exposure represented the level of sucrose preference post LAN treatment.

**Novelty Seeking.** All novelty-seeking tests were performed between 10 am and 2 pm when the animals were most active, following the previously described procedures (35, 37). During the test, we hung a novel object that the animals had never seen in the corner of the cage. The activities of the tree shrews were monitored for 10 min using a video recorder installed on the top of the cage. Then, the frequency of visits to the novelty-seeking area (a square area centered

around the novel object with a side length of 30 cm) was counted by the observer (same one throughout the study). Some tree shrews were excluded from further experiments because they did not visit the novelty-seeking area during baseline assessments.

**Rhythmic Activity.** Three tree shrews were randomly selected from each group for the evaluation of circadian activity rhythm. An infrared video camera was used to record the locomotor activities of the tree shrews for five consecutive days. Videos were analyzed using Ethovision software (v.XT 8.5) to measure the duration in the activity area. From ZT1 to ZT11, the activity duration during a 10-min period in the middle of each hour was measured, and then multiplied by six to represent hourly activity. From ZT12 to ZT24, activity duration in the whole hour was analyzed. Total time spent in the activity area at each timepoint was averaged across three animals and five sampling days, and the results were used to represent the activity level of tree shrews at different times of the day.

**Hole-Board Task.** The hole-board was made of black cardboard (297 × 105 mm), with ten holes (diameter 15 mm) staggered in three rows, following the procedure in our recent study (37). The detailed operational steps for the habituation and training phases are provided in the *SI Appendix, Supplement Materials and Methods*. The detection phase was conducted at 1 h, 24 h, and 96 h after the termination of the training phase, without yellow mealworms in any of the holes. The whole experiment was recorded. Throughout the experiment, the hole-boards were wiped with alcohol after each trial to eliminate odor. Some tree shrews were excluded from further experiments because they could not complete the task during the latter 2 d of the training phase before LAN.

During the detection phase, the total time taken by the tree shrews to complete the task (successfully locate all three targets) was recorded, referred to as  $T_{\text{total}}$ . Efficiency was defined as  $(300 \text{ s} - T_{\text{total}})/300 \text{ s} \times 100\%$ . The number of wrong choices (attempts made to open nontarget holes before all three target holes were found) was counted by the same observer throughout the study.

**RNA-Sequencing Analysis.** Two tree shrews were randomly selected from each group, and quickly killed under deep anesthesia between 2 pm and 4 pm. Brain tissues were removed and placed in cold (0 to 4 °C) cutting solution containing (in mM): 92 NMDG, 1.2 KCl, 1.2 KH<sub>2</sub>PO<sub>4</sub>, 30 NaHCO<sub>3</sub>, 25 d-glucose, 3 Na-pyruvate, 5 l-ascorbic acid, 2 thiourea, 10 MgSO<sub>4</sub>, 20 HEPES, 0.5 CaCl<sub>2</sub>, adjusted to pH = 7.3 using HCl, 300 to 310 mOsm. Coronal slices (900 μm thick) were made on a vibrating microtome (Leica VT-1200S). The NAc was excised and placed in RNAlater solution (Thermo Fisher AM7021) and stored at –80 °C. The samples were sent to Berry Genomics (Beijing) for RNA-sequencing.

**Differential Gene Expression Analysis.** FASTQ sequences were mapped to the tree shrew genome ver 3.0 (42), which was downloaded from the tree shrew database website (<http://www.treeshrewdb.org/download.html>) and aligned using

STAR (63). After acquiring the expression matrix, differential expression analysis was conducted using the DESeq2 (64) package for R. Differentially expressed genes were identified by applying the Benjamini-Hochberg procedure to adjust for multiple comparisons, with an adjusted *P* value threshold set at <0.05 for false discovery rate, and  $|\log_{2}\text{foldchange}| > 1$ .

**Gene Set Enrichment Analysis.** The gene matrix [ $\log_{2}$  foldchange (CT/EX)] was arranged in descending order and then the R package GSEAbase was used to calculate the enrichment score and *P* value of the gene set of pathway downloaded from MSigDB (65) in the gene matrix. A significance threshold of *P* < 0.05 was applied to identify significantly enriched pathways.

**Statistics Reproducibility.** Data were presented as the means ± SEMs. No statistical methods were used to predetermine sample sizes. Sample sizes are indicated in the figures' legends and associated text. Statistical differences were determined using a paired or unpaired two-tailed *t* test, or with two-way ANOVA statistical tests, followed by Tukey's post hoc test. *P* values less than 0.05 were considered to be statistically significant. *P* values were indicated as follows: \**P* < 0.05, \*\**P* < 0.01; \*\*\**P* < 0.001; ns, not significant.

**Data, Materials, and Software Availability.** The raw RNA-seq data used in this study have been deposited in our laboratory database and are available at Genome Sequence Archive (GSA) under the accession number CRA025777 (66). All other data are included in the article and/or *SI Appendix*.

**ACKNOWLEDGMENTS.** We thank the funding of National Key Research and Development Program of China (2020YFA0112200) and STI2030-Major Projects (2021ZD0200900), Research Programs of the Chinese Academy of Sciences (XDB39050300, YSBR-013, xbgz-zdys-202302), The Feng Foundation of Biomedical Research, National Natural Science Foundation of China (81925009, 32121002, 32371056), Anhui Provincial Natural Science Foundation (2308085MH282), and Yunnan Province (202305AH340006).

Author affiliations: <sup>a</sup>Hefei National Research Center for Physical Sciences at the Microscale, Chinese Academy of Sciences Key Laboratory of Brain Function and Disease, Biomedical Sciences and Health Laboratory of Anhui Province, School of Life Sciences, Division of Life Sciences and Medicine, University of Science and Technology of China, Hefei 230026, China; <sup>b</sup>Key Laboratory of Genetic Evolution and Animal Models of the Chinese Academy of Sciences, Key Laboratory of Animal Models and Human Disease Mechanisms of Yunnan Province, and Kunming Institute of Zoology and Chinese University of Hong Kong Joint Laboratory of Bioresources and Molecular Research in Common Diseases, Kunming Institute of Zoology, Chinese Academy of Sciences, Kunming, Yunnan 650204, China; <sup>c</sup>School of Biology, Food, and Environment, Department of Biological Engineering, Hefei University, Hefei, Anhui 230601, China; <sup>d</sup>National Research Facility for Phenotypic and Genetic Analysis of Model Animals (Primate Facility), National Resource Center for Non-Human Primates, Kunming Institute of Zoology, Chinese Academy of Sciences, Kunming, Yunnan 650107, China; and <sup>e</sup>Kunming College of Life Science, University of Chinese Academy of Sciences, Kunming, Yunnan 650204, China

1. C. S. Pittendrigh, Temporal organization: Reflections of a Darwinian clock-watcher. *Annu. Rev. Physiol.* **55**, 16–54 (1993), 10.1146/annurev.ph.55.030193.000313.
2. S. M. Reppert, D. R. Weaver, Coordination of circadian timing in mammals. *Nature* **418**, 935–941 (2002), 10.1038/nature00965.
3. U. Albrecht, J. A. Ripperger, Circadian clocks and sleep: Impact of rhythmic metabolism and waste clearance on the brain. *Trends Neurosci.* **41**, 677–688 (2018), 10.1016/j.tins.2018.07.007.
4. K. L. Gamble, R. Berry, S. J. Frank, M. E. Young, Circadian clock control of endocrine factors. *Nat. Rev. Endocrinol.* **10**, 466–475 (2014), 10.1038/nrendo.2014.78.
5. H. Reinke, G. Asher, Crosstalk between metabolism and circadian clocks. *Nat. Rev. Mol. Cell Biol.* **20**, 227–241 (2019), 10.1038/s41580-018-0096-9.
6. R. W. Logan, D. K. Sarkar, Circadian nature of immune function. *Mol. Cell. Endocrinol.* **349**, 82–90 (2012), 10.1016/j.mce.2011.06.039.
7. M. J. Boden, D. J. Kennaway, Circadian rhythms and reproduction. *Reproduction* **132**, 379–392 (2006), 10.1530/rep.0.00614.
8. J. Bass, M. A. Lazar, Circadian time signatures of fitness and disease. *Science* **354**, 994–999 (2016), 10.1126/science.aaa4965.
9. J. J. Meng *et al.*, Light modulates glucose metabolism by a retina-hypothalamus-brown adipose tissue axis. *Cell* **186**, 398–412.e17 (2023), 10.1016/j.cell.2022.12.024.
10. J. Hu *et al.*, Melanopsin retinal ganglion cells mediate light-promoted brain development. *Cell* **185**, 3124–3137.e15 (2022), 10.1016/j.cell.2022.07.009.
11. D. C. Fernandez *et al.*, Light affects mood and learning through distinct retina-brain pathways. *Cell* **175**, 71–84.e18 (2018), 10.1016/j.cell.2018.08.004.
12. G. Vandewalle, P. Maquet, D. J. Dijk, Light as a modulator of cognitive brain function. *Trends Cogn. Sci.* **13**, 429–438 (2009), 10.1016/j.tics.2009.07.004.
13. J. R. Bumgarner, R. J. Nelson, Light at night and disrupted circadian rhythms alter physiology and behavior. *Integr. Comp. Biol.* **61**, 1160–1169 (2021), 10.1093/icb/icab017.
14. Y. Cho *et al.*, Effects of artificial light at night on human health: A literature review of observational and experimental studies applied to exposure assessment. *Chronobiol. Int.* **32**, 1294–1310 (2015), 10.3109/07420528.2015.1073158.
15. G. Muscogiuri *et al.*, Exposure to artificial light at night: A common link for obesity and cancer? *Eur. J. Cancer* **173**, 263–275 (2022), 10.1016/j.ejca.2022.06.007.
16. Y. X. Xu, J. H. Zhang, F. B. Tao, Y. Sun, Association between exposure to light at night (LAN) and sleep problems: A systematic review and meta-analysis of observational studies. *Sci. Total Environ.* **857**, 159303 (2023), 10.1016/j.scitotenv.2022.159303.
17. A. Haim, A. E. Zubidat, Artificial light at night: Melatonin as a mediator between the environment and epigenome. *Philos. Trans. R. Soc. Lond. B Biol. Sci.* **370**, 20140121 (2015), 10.1098/rstb.2014.0121.
18. S. Tancredi, T. Urbano, M. Vinceti, T. Filippini, Artificial light at night and risk of mental disorders: A systematic review. *Sci. Total Environ.* **833**, 155185 (2022), 10.1016/j.scitotenv.2022.155185.
19. L. Yan, J. S. Lonstein, A. A. Nunez, Light as a modulator of emotion and cognition: Lessons learned from studying a diurnal rodent. *Horm. Behav.* **111**, 78–86 (2019), 10.1016/j.yhbeh.2018.09.003.
20. T. A. Bedrosian, R. J. Nelson, Timing of light exposure affects mood and brain circuits. *Transl. Psychiatry* **7**, e1017 (2017), 10.1038/tp.2016.262.
21. T. A. LeGates *et al.*, Aberrant light directly impairs mood and learning through melanopsin-expressing neurons. *Nature* **491**, 594–598 (2012), 10.1038/nature11673.
22. K. An *et al.*, A circadian rhythm-gated subcortical pathway for nighttime-light-induced depressive-like behaviors in mice. *Nat. Neurosci.* **23**, 869–880 (2020), 10.1038/s41593-020-0640-8.
23. L. K. Fonken, E. Kitsmiller, L. Smale, R. J. Nelson, Dim nighttime light impairs cognition and provokes depressive-like responses in a diurnal rodent. *J. Biol. Rhythms* **27**, 319–327 (2012), 10.1177/0748730412448324.
24. L. Yan, L. Smale, A. A. Nunez, Circadian and photic modulation of daily rhythms in diurnal mammals. *Eur. J. Neurosci.* **51**, 551–566 (2020), 10.1111/ejn.14172.

25. L. Smale, T. Lee, A. A. Nunez, Mammalian diurnality: Some facts and gaps. *J. Biol. Rhythms* **18**, 356–366 (2003), 10.1177/0748730403256651.

26. J. Mendoza, Nighttime light hurts mammalian physiology: What diurnal rodent models are telling us. *Clocks Sleep* **3**, 236–250 (2021), 10.3390/clocksleep3020014.

27. C. Bilu, H. Einat, N. Kronfeld-Schor, Utilization of diurnal rodents in the research of depression. *Drug Dev. Res.* **77**, 336–345 (2016), 10.1002/ddr.21346.

28. S. K. T. Taufique, A. Prabhat, V. Kumar, Illuminated night alters hippocampal gene expressions and induces depressive-like responses in diurnal corvids. *Eur. J. Neurosci.* **48**, 3005–3018 (2018), 10.1111/ejn.14157.

29. J. Wang *et al.*, Washed microbiota transplantation accelerates the recovery of abnormal changes by light-induced stress in tree shrews. *Front. Cell. Infect. Microbiol.* **11**, 685019 (2021), 10.3389/fcimb.2021.685019.

30. J. E. Janecka *et al.*, Molecular and genomic data identify the closest living relative of primates. *Science* **318**, 792–794 (2007), 10.1126/science.1147555.

31. Y. G. Yao, Creating animal models, why not use the Chinese tree shrew (*Tupaia belangeri chinensis*)? *Zool. Res.* **38**, 118–126 (2017), 10.24272/j.issn.2095-8137.2017.032.

32. Y. Fan *et al.*, Chromosomal level assembly and population sequencing of the Chinese tree shrew genome. *Zool. Res.* **40**, 506–521 (2019), 10.24272/j.issn.2095-8137.2019.063.

33. Y. G. Yao *et al.*, Study of tree shrew biology and models: A booming and prosperous field for biomedical research. *Zool. Res.* **45**, 877–909 (2024), 10.24272/j.issn.2095-8137.2024.199.

34. E. Savier, M. Sedigh-Sarvestani, R. Wimmer, D. Fitzpatrick, A bright future for the tree shrew in neuroscience research: Summary from the inaugural Tree Shrew Users Meeting. *Zool. Res.* **42**, 478–481 (2021), 10.24272/j.issn.2095-8137.2021.178.

35. F. Shen *et al.*, Differential effects of clomipramine on depression-like behaviors induced by the chronic social defeat paradigm in tree shrews. *J. Psychopharmacol.* **32**, 1141–1149 (2018), 10.1177/0269881118793560.

36. B. Schmelting *et al.*, Agomelatine in the tree shrew model of depression: Effects on stress-induced nocturnal hyperthermia and hormonal status. *Eur. Neuropsychopharmacol.* **24**, 437–447 (2014), 10.1016/j.euroneuro.2013.07.010.

37. H. Li *et al.*, Cognitive deficits and Alzheimer's disease-like pathologies in the aged Chinese tree shrew. *Mol. Neurobiol.* **61**, 1892–1906 (2024), 10.1007/s12035-023-03663-7.

38. C. R. Pryce, E. Fuchs, Chronic psychosocial stressors in adulthood: Studies in mice, rats and tree shrews. *Neurobiol. Stress* **6**, 94–103 (2017), 10.1016/j.jnstr.2016.10.001.

39. H. Fang *et al.*, High activity of the stress promoter contributes to susceptibility to stress in the tree shrew. *Sci. Rep.* **6**, 24905 (2016), 10.1038/srep24905.

40. E. Fuchs, M. Kramer, B. Hermes, P. Netter, C. Hiemke, Psychosocial stress in tree shrews: Clomipramine counteracts behavioral and endocrine changes. *Pharmacol. Biochem. Behav.* **54**, 219–228 (1996), 10.1016/0091-3057(95)02166-3.

41. E. Fuchs, G. Flügge, Social stress in tree shrews: Effects on physiology, brain function, and behavior of subordinate individuals. *Pharmacol. Biochem. Behav.* **73**, 247–258 (2002), 10.1016/s0091-3057(02)00795-5.

42. M. S. Ye *et al.*, Comprehensive annotation of the Chinese tree shrew genome by large-scale RNA sequencing and long-read isoform sequencing. *Zool. Res.* **42**, 692–709 (2021), 10.24272/j.issn.2095-8137.2021.272.

43. J. Karska *et al.*, Artificial light and neurodegeneration: Does light pollution impact the development of Alzheimer's disease? *Geroscience* **46**, 87–97 (2024), 10.1007/s11357-023-00932-0.

44. T. A. LeGates, D. C. Fernandez, S. Hattar, Light as a central modulator of circadian rhythms, sleep and affect. *Nat. Rev. Neurosci.* **15**, 443–454 (2014), 10.1038/nrn3743.

45. L. Huang *et al.*, A visual circuit related to habenula underlies the antidepressive effects of light therapy. *Neuron* **102**, 128–142.e28 (2019), 10.1016/j.neuron.2019.01.037.

46. C. A. Palmer *et al.*, Sleep loss and emotion: A systematic review and meta-analysis of over 50 years of experimental research. *Psychol. Bull.* **150**, 440–463 (2024), 10.1037/bul0000410.

47. E. J. Nestler, Role of the brain's reward circuitry in depression: Transcriptional mechanisms. *Int. Rev. Neurobiol.* **124**, 151–170 (2015), 10.1016/bs.irn.2015.07.003.

48. T. T. Pan *et al.*, Nucleus accumbens-linked executive control networks mediating reversal learning in tree shrew brain. *Zool. Res.* **43**, 528–531 (2022), 10.24272/j.issn.2095-8137.2022.063.

49. H. Carceller, Y. Gramuntell, P. Klimczak, J. Nacher, Perineuronal nets: Subtle structures with large implications. *Neuroscientist* **29**, 569–590 (2023), 10.1177/10738584221106346.

50. J. W. Fawcett, T. Oohashi, T. Pizzorusso, The roles of perineuronal nets and the perinodal extracellular matrix in neuronal function. *Nat. Rev. Neurosci.* **20**, 451–465 (2019), 10.1038/s41583-019-0196-3.

51. J. C. Morphett, A. L. Whittaker, A. C. Reichelt, M. R. Hutchinson, Perineuronal net structure as a non-cellular mechanism contributing to affective state: A scoping review. *Neurosci. Biobehav. Rev.* **158**, 105568 (2024), 10.1016/j.neubiorev.2024.105568.

52. M. F. Hazlett *et al.*, The perineuronal net protein brevican acts in nucleus accumbens parvalbumin-expressing interneurons of adult mice to regulate excitatory synaptic inputs and motivated behaviors. *Biol. Psychiatry* **96**, 694–707 (2024), 10.1016/j.biopsych.2024.02.003.

53. Y. Zhang *et al.*, Possible involvement of perineuronal nets in anti-depressant effects of electroacupuncture in chronic-stress-induced depression in rats. *Neurochem. Res.* **48**, 3146–3159 (2023), 10.1007/s11064-023-03970-4.

54. Y. P. López-Echeverri, K. J. Cardona-Londoño, J. F. García-Aguirre, M. Orrego-Cardozo, Effects of serotonin transporter and receptor polymorphisms on depression. *Rev. Colomb. Psiquiatr. (Engl. Ed)* **52**, 130–138 (2023), 10.1016/j.rcpeng.2021.07.003.

55. I. J. You *et al.*, 5-HT1A autoreceptors in the dorsal raphe nucleus convey vulnerability to compulsive cocaine seeking. *Neuropsychopharmacology* **41**, 1210–1222 (2016), 10.1038/npp.2015.268.

56. Z. Ercan *et al.*, Treadmill exercise improves behavioral and neurobiological alterations in restraint-stressed rats. *J. Mol. Neurosci.* **73**, 831–842 (2023), 10.1007/s12031-023-02159-2.

57. J.-N. Zhou, R.-J. Ni, *The Tree Shrew (*Tupaia belangeri chinensis*) Brain in Stereotaxic Coordinates* (Springer, 2016).

58. E. Fuchs, Social stress in tree shrews as an animal model of depression: An example of a behavioral model of a CNS disorder. *CNS Spectr.* **10**, 182–190 (2005), 10.1017/s1092852900010038.

59. M. Sedigh-Sarvestani *et al.*, A sinusoidal transformation of the visual field is the basis for periodic maps in area V2. *Neuron* **109**, 4068–4079.e66 (2021), 10.1016/j.neuron.2021.09.053.

60. D. Familtsev *et al.*, Ultrastructure of geniculocortical synaptic connections in the tree shrew striate cortex. *J. Comp. Neurol.* **524**, 1292–1306 (2016), 10.1002/cne.23907.

61. A. Parra, C. A. Baker, M. M. Bolton, Regional specialization of pyramidal neuron morphology and physiology in the tree shrew neocortex. *Cereb. Cortex* **29**, 4488–4505 (2019), 10.1093/cercor/bhy326.

62. J. Wang *et al.*, Chronic clomipramine treatment reverses core symptoms of depression in subordinate tree shrews. *PLoS One* **8**, e80980 (2013), 10.1371/journal.pone.0080980.

63. A. Dobin *et al.*, STAR: Ultrafast universal RNA-seq aligner. *Bioinformatics* **29**, 15–21 (2013), 10.1093/bioinformatics/bts635.

64. M. I. Love, W. Huber, S. Anders, Moderated estimation of fold change and dispersion for RNA-seq data with DESeq2. *Genome Biol.* **15**, 550 (2014), 10.1186/s13059-014-0550-8.

65. A. Liberzon *et al.*, Molecular signatures database (MSigDB) 3.0. *Bioinformatics* **27**, 1739–1740 (2011), 10.1093/bioinformatics/btr260.

66. Y. Miao *et al.*, Transcriptome (RNA-seq) data of the nucleus accumbens in tree shrews. GSA. <https://ngdc.cncb.ac.cn/gsa/browse/CRA025777>. Deposited 16 May 2025.

## Supporting Information for

### Light-at-night negatively affects mood in diurnal primate-like tree shrews via a visual pathway related to the perihabenular nucleus

Ying Miao<sup>1,2†</sup>, Huan Zhao<sup>3†\*</sup>, Yu-Fei Li<sup>1†</sup>, Yan-Ping Sun<sup>1</sup>, Rui Bi<sup>2,4,5</sup>, Hong-Li Li<sup>2,4</sup>, Xin Fang<sup>1</sup>, Zi-Shuo Li<sup>1</sup>, Yu-Hua Ma<sup>4</sup>, Long-Bao Lv<sup>2,4</sup>, Kai An<sup>1</sup>, Jian-Jun Meng<sup>1\*</sup>, Yong-Gang Yao<sup>2,4,5\*</sup>, Tian Xue<sup>1\*</sup>

<sup>1</sup> Hefei National Research Center for Physical Sciences at the Microscale, CAS Key Laboratory of Brain Function and Disease, Biomedical Sciences and Health Laboratory of Anhui Province, School of Life Sciences, Division of Life Sciences and Medicine, University of Science and Technology of China, Hefei 230026, China

<sup>2</sup> Key Laboratory of Genetic Evolution and Animal Models of the Chinese Academy of Sciences, Key Laboratory of Animal Models and Human Disease Mechanisms of Yunnan Province, and KIZ-CUHK Joint Laboratory of Bioresources and Molecular Research in Common Diseases, Kunming Institute of Zoology, Chinese Academy of Sciences, Kunming, Yunnan 650204, China

<sup>3</sup> School of Biology, Food, and Environment, Hefei University, Hefei, Anhui 230601, China

<sup>4</sup> National Research Facility for Phenotypic & Genetic Analysis of Model Animals (Primate Facility), National Resource Center for Non-Human Primates, Kunming Institute of Zoology, Chinese Academy of Sciences, Kunming, Yunnan 650107, China

<sup>5</sup> Kunming College of Life Science, University of Chinese Academy of Sciences, Kunming, Yunnan 650204, China

<sup>†</sup> These authors contributed equally to this work

<sup>\*</sup> Corresponding authors:

Huan Zhao; Email: [hzhao@hfuu.edu.cn](mailto:hzhao@hfuu.edu.cn);

Jian-jun Meng; Email: [jianjunm@ustc.edu.cn](mailto:jianjunm@ustc.edu.cn);

Yong-Gang Yao; Email: [yaoyg@mail.kiz.ac.cn](mailto:yaoyg@mail.kiz.ac.cn);

Tian Xue; Email: [xuetian@ustc.edu.cn](mailto:xuetian@ustc.edu.cn)

**This PDF file includes:**

Supplement Materials and Methods  
Figures S1 to S6

## **Supplement Materials and Methods**

### **Anterograde and retrograde tracers and viruses**

This study employed the following fluorescent tracing dyes and viral tools: Alexa fluor 555-conjugated cholera toxin subunit B (CTB-555, Thermo Fisher c34776) and CTB-488 (BrainVTA) were used for anterograde or retrograde tracing.. AAV1-Cre(scAAV2/1-hSyn-Cre-pA) was used to express Cre recombinase in postsynaptic neurons to achieve input-specific labeling. AAV2/9-EF1a-DIO-ChR2-EGFP and AAV2/9-CAG-FLEX-EGFP were used to Cre-dependently express Green fluorescent protein in central neurons, while AAV2/2-hSyn-DIO-mCherry was used to Cre-dependently express mCherry fluorescent protein in retinal ganglion cells. AAV2/9-CAG-FLEX-EGFP was obtained from OBiO Technology(Shanghai)Corp.,Ltd. All other AAV tools were prepared by Shanghai Taitool Bioscience.

### **Antibody**

The primary antibodies used in the current study were as follows: rabbit anti-cFos (Synaptic Systems 226008; 1:5000; lot no. 1-27); rabbit anti-NEUN (Proteintech 26975-1-AP; 1:500; lot no. 00143425). The following secondary antibodies were used in this study: Alexa Fluor 488 (Thermo Fisher A-11034; 1:500; lot no. 2069632).

### **Body weight**

Tree shrews were weighed in the morning by restraining them in a pouch, and the actual body weight of each animal was recorded (after subtracting the weight of the pouch).

### **Locomotion activity**

The movements of the tree shrews were tracked for 1 h (conducted between 10 am and 2 pm) by a video recorder installed atop the cage. Videos were analyzed using Ethovision software (v.XT 8.5) to measure the duration in the cage and distance moved. The number of jumps within the cage and the number of crossings between the nesting box and the activity area of the cage were counted by the observer.

### **Rhythmic activity**

For experiments in supplementary figure 1E-G, we first maintained all animals under 12L:12D for three weeks after habituation. At the end of the three weeks, we switched animals to constant dark conditions (D/D) for one day to obtain body temperature and locomotion data without the masking effect (12/12 D/D). After that, animals were semi-randomly split into two groups, one kept under LAN conditions and the other under 15L:9D conditions to mimic extended days. Then, after another three weeks, we switched all animals to constant darkness again and obtained body temperature and locomotion data. Infrared cameras were employed to monitor behavior in activity

cages continuously. Video recordings from ZT9 to ZT16 were analyzed. The duration of the tree shrew staying in the activity cage was manually counted and plotted at a bin value of 10 minutes.

### **Body temperature**

Tree shrews were implanted with thermo-loggers subcutaneously in the dorsal region as advised by the manufacturer (Shenzhen Flamingo Technology Co., Ltd.). In brief, animals were anesthetized, and a section of dorsal skin was shaved and sterilized. A skin incision was made, and the connective tissue between the skin and underlying muscle layer was gently separated. Pre-activated thermo-loggers that had been surface-sterilized with 75% ethanol were inserted into the subcutaneous pocket and sutured. Following their recovery from anesthesia, the animals were returned to their home cages. Body temperature recordings commenced after a 24-hour recovery period. Body temperature data from tree shrews were normalized by defining the average value during ZT9–ZT11 as 100% and the average value during ZT14–ZT16 as 0%. Normalized body temperatures were plotted at a bin value of 5 minutes. The 50% cutoff values obtained from fitted BT curves (ZT9–ZT16 interval), calculated as the time at which BT reached 50% of the reduction from its daily maximum value.

### **Analysis of blood hormone**

Approximately 1 mL of blood was collected from the tree shrews' femoral vein between 8 am and 10 am. The collected whole blood was left to stand at room temperature for 60 min, followed by centrifugation at 3000Xg for 10 min. The supernatant was collected and immediately frozen in liquid nitrogen and stored at -80 °C. Serum samples (0.3-0.5 mL) were sent to Shanghai Zhongke New Life Biotechnology Co. Ltd. for assessments. Selected steroid hormones were measured using high-performance liquid chromatography-tandem mass spectrometry (LC-MS/MS) based on their common protocol for commercial service.

### **Habituation and training procedures for the hole-board task**

During the habituation period, all holes were exposed and baited with yellow mealworms. Then hole-boards were placed inside the cages to attract the tree shrews to feed on the yellow mealworms and to alleviate their fear of the unfamiliar hole-boards. Subsequently, tree shrews were given hole-boards with all holes covered with loose lids, and needed to learn to open the lids of the holes to obtain yellow mealworms. After all tree shrews became proficient, the experiment commenced with a training phase from the 1st day to the 3rd day. During this phase, three out of the ten holes were designated as target holes each day and labeled with yellow rectangular tags. The remaining seven holes served as distractor holes and were labeled with blue triangular tags. The arrangement of the target holes was changed daily, with three different layouts. Only the target holes were loaded with yellow mealworms to progressively train the tree shrews to distinguish the target labels. The training was repeated three times daily.

After LAN exposure, in order to minimize interference from learning experiences, target holes were designated with green X-shaped markers, while distractor holes were labeled with orange square tags.

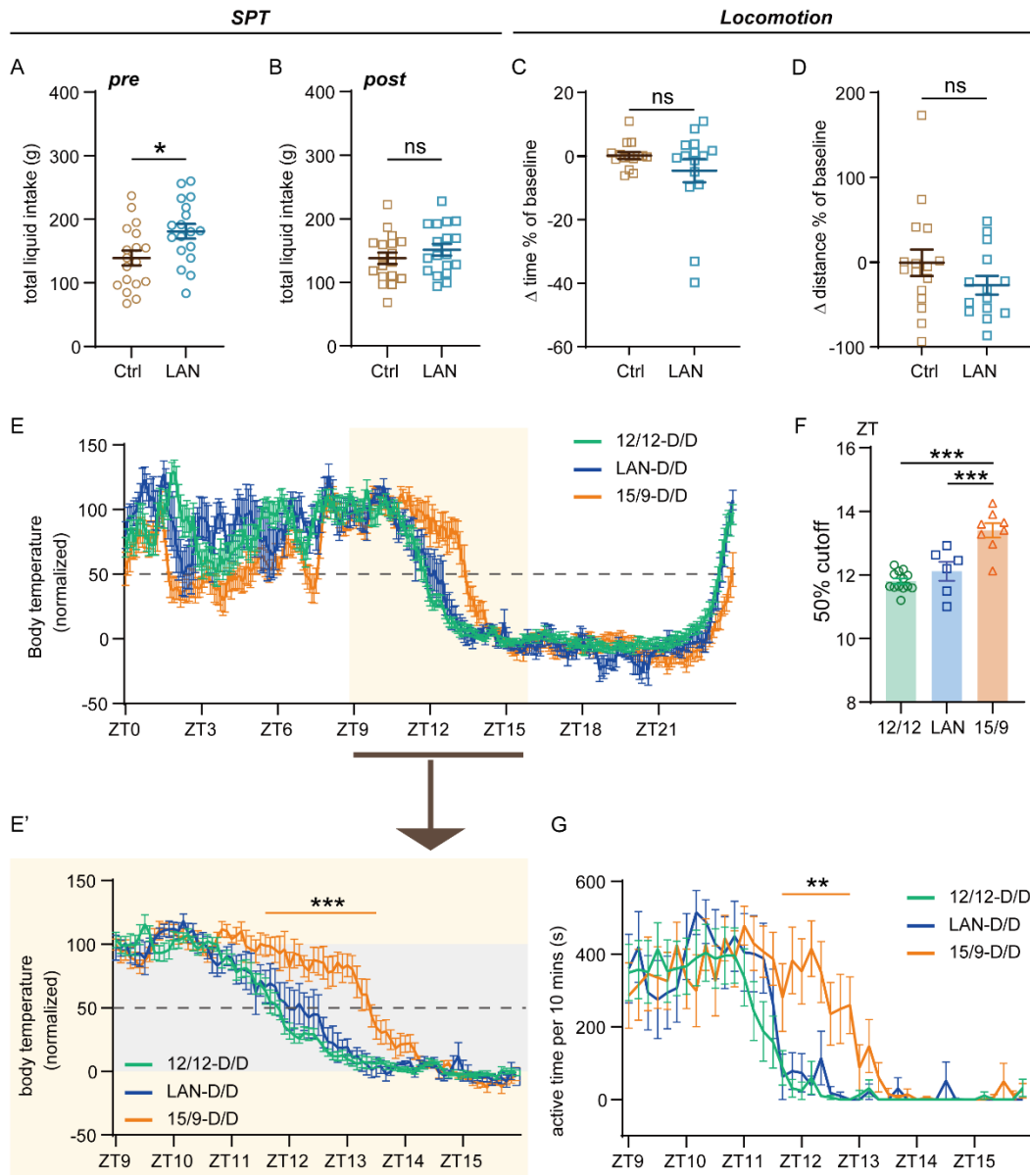


**Figure S1. LAN exposure does not affect locomotion and circadian phase**

**A-B**, Before LAN exposure (*pre*), in the sucrose preference test (SPT), the total liquid intake of the LAN group was mildly but significantly higher than the Ctrl group (**A**) ( $n=18$  tree shrews,  $P<0.05$ , two-tailed unpaired t-test). No significant difference after LAN exposure (**B**) ( $n=18$  tree shrews,  $P>0.05$ , two-tailed unpaired t-test).

**C-D**, No difference was observed in the percentage change of locomotion time (**C**) (Ctrl,  $n = 15$ ; LAN,  $n=15$ ,  $P>0.05$ , two-tailed unpaired t-test) and distance (**D**) (Ctrl,  $n=16$ , LAN,  $n=14$ ,  $P>0.05$ , two-tailed unpaired t-test) between the Ctrl and LAN groups of tree shrews.

**E**, Normalized body temperatures in tree shrews in constant darkness (D/D) following 3-wk exposure to different photoperiods. Whole-day fluctuations from all three groups are shown above, while data between ZT9 and ZT16 are replotted below for a better display of details. (12L/12D, green,  $n=14$ ; 15L/9D, orange,  $n=8$ ; LAN, blue,  $n=6$  tree shrews). The horizontal bar

above the plots indicates the period when 15/9-D/D is statistically significantly different from LAN-D/D and 12/12-D/D, while LAN-D/D and 12/12-D/D are not statistically different (by multiple comparisons). Data were analyzed using Two-way ANOVA with Tukey's multiple comparisons test,  $F (166, 2100) = 4.914$ ,  $P < 0.0001$ .

**F**, Body temperature data of tree shrews from different groups between ZT9 and ZT16 were fitted to determine the 50% cutoff time (inflection point of the sigmoidal curve) for each individual. (12/12, green,  $n=13$ ; 15/9, orange,  $n=8$ ; LAN, blue,  $n=6$  tree shrews). 15/9 is statistically significantly different from LAN and 12/12, while LAN and 12/12 are not statistically different (by multiple comparisons). Data were analyzed using One-way ANOVA with Tukey's multiple comparisons test,  $F (2, 24) = 23.32$ ,  $P < 0.0001$ .

**G**, Locomotion patterns during ZT9–ZT16 in tree shrews in constant darkness (D/D) following 3-wk exposure to different photoperiods. (12L/12D, green,  $n=10$ , 15L/9D, orange,  $n=8$ , LAN, blue,  $n=7$  tree shrews). The horizontal bar above the plots indicates the period when 15/9-D/D is statistically significantly different from LAN-D/D and 12/12-D/D, while LAN-D/D and 12/12-D/D are not statistically different (by multiple comparisons). Data were analyzed using Two-way ANOVA with Tukey's multiple comparisons test,  $F (82, 924) = 1.695$ ,  $P = 0.0002$ .

Values are presented as mean  $\pm$  s.e.m. ns, not significant, \*,  $P < 0.05$ ; \*\*,  $P < 0.01$ ; \*\*\*,  $P < 0.0001$ ;

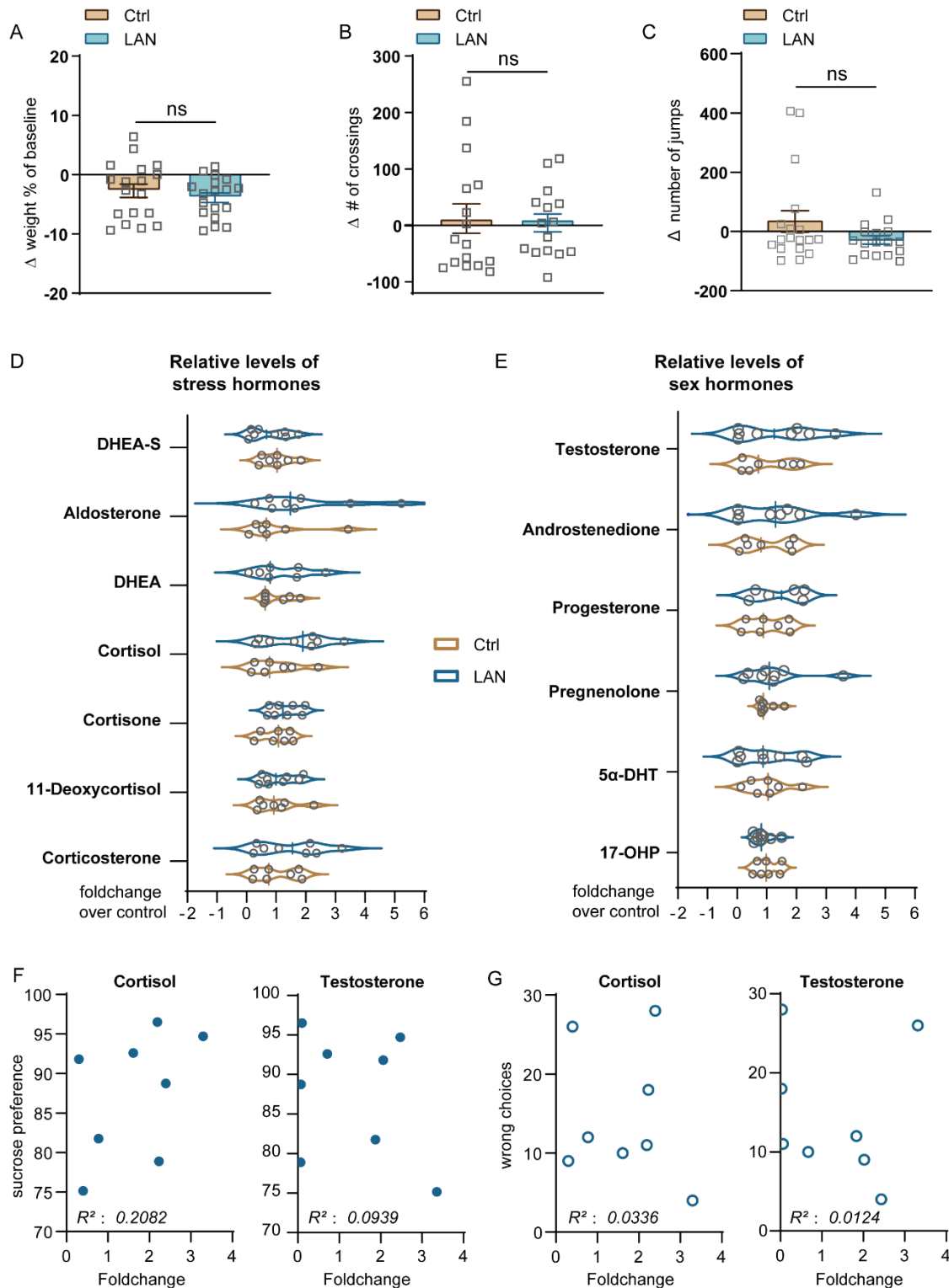


**Figure S2. LAN exposure does not evoke anxiety-like behaviors or stress responses.**

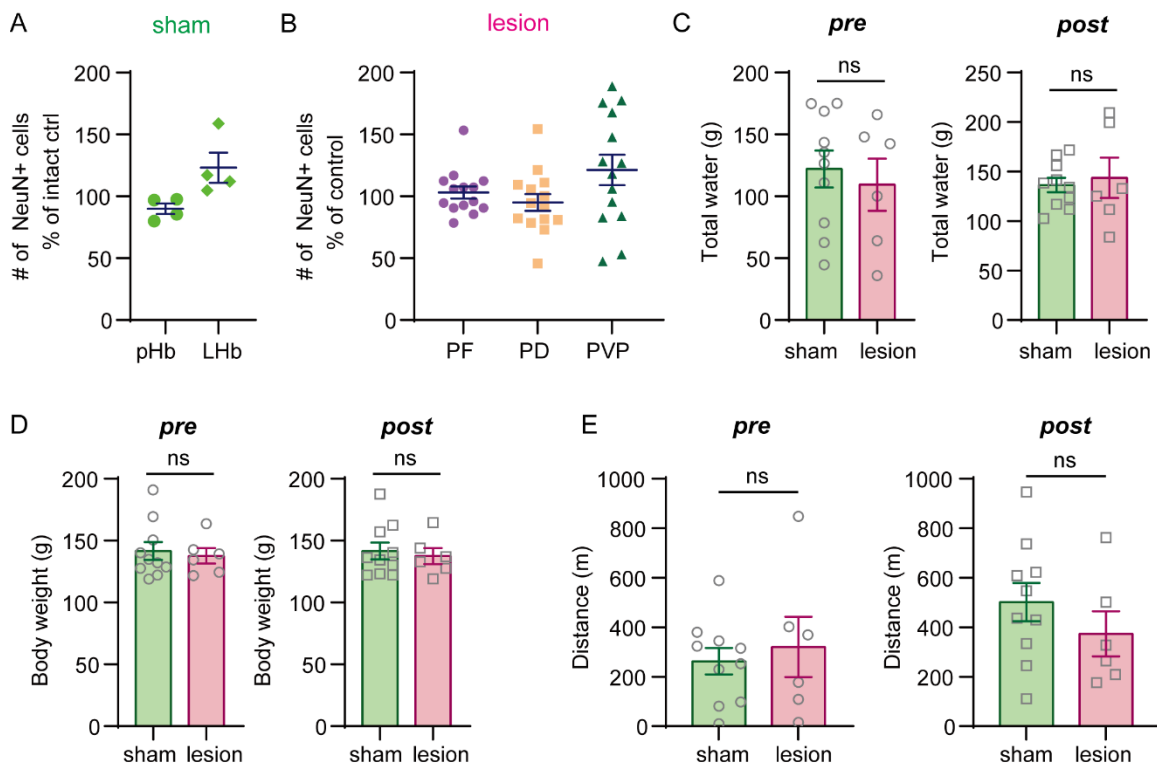
**A**, The percentage of body-weight change after the modeling period relative to baseline was not statistically different between Ctrl and LAN groups (n=18 tree shrews per group; P>0.05, two-tailed unpaired t-test).

**B,C**, No significant differences in the number of crossings (**B**) (Ctrl, n=16 tree shrews, LAN, n = 15 tree shrews; P >0.05, two-tailed unpaired t-test) and jumps (**C**) (Ctrl, n=18 tree shrews, LAN, n=17 tree shrews; P>0.05, two-tailed unpaired t-test) after the modeling period relative to baseline between the two groups of tree shrews.

**D,E**, In the control and LAN-exposed animals, the relative plasma levels of stress hormones (**D**) and sex hormones (**E**) were not statistically significantly different (Ctrl, n=7 tree shrews; LAN, n=8 tree shrews). The plasma level of each hormone was normalized to the average level of the control animals and expressed as fold change over control.

**F,G**, The relative plasma levels of cortisol and testosterone do not correlate with behavioral changes in the sucrose preference test (**F**) and Hole-board task (**G**). The correlation index  $R^2$  was marked at the lower left corner.

Values are presented as mean  $\pm$  s.e.m. ns, not significant.



Values are presented as mean  $\pm$  s.e.m. ns, not significant; two-tailed unpaired t-test.

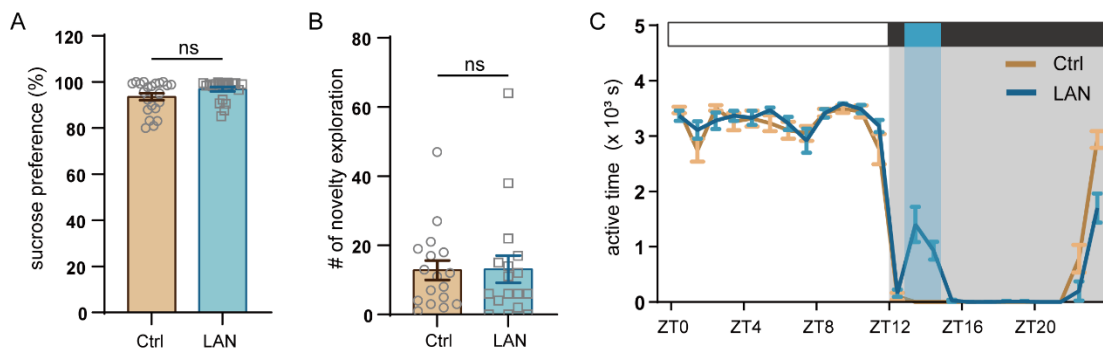


**Figure S4. LAN fails to affect emotion with pHb lesion.**

**A**, Sucrose preference of tree shrews with pHb lesion was not significantly different before (Ctrl; orange) and after the LAN exposure (LAN; blue) ( $n=22$  tree shrews,  $P>0.05$ , two-tailed paired t-test).

**B**, The numbers of explorations of novel objects were not significantly different in tree shrews with pHb-lesion before and after LAN treatment ( $n=17$  tree shrews,  $P>0.05$ , two-tailed paired t-test).

**C**, The hourly active duration of tree shrews before the experiment (Ctrl) and under LAN conditions (LAN) ( $n=3$  tree shrews).

Values are presented as mean  $\pm$  s.e.m. ns, not significant; two-tailed paired t-test.

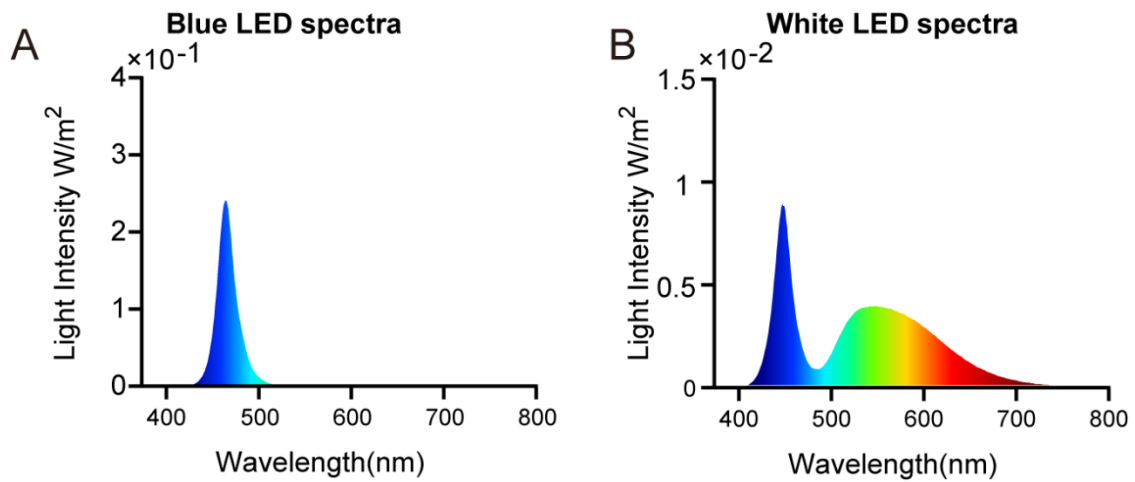


**Figure S5. The spectrum properties of the blue and white LED illumination used in the current study**

**A**, The spectrum of blue LED light.

**B**, The spectrum of white LED light.

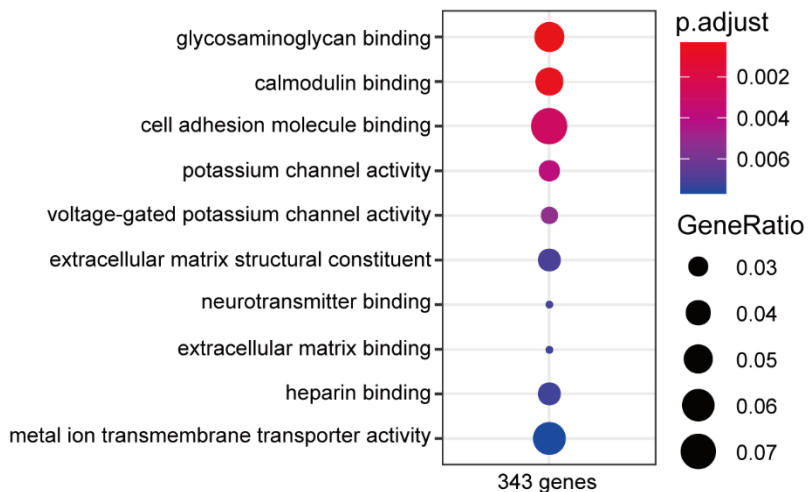


**Figure S6. Gene ontology enrichment analysis of differentially expressed genes in NAc tissues of the tree shrews with or without LAN exposure.**

Dot plot for the Gene ontology (GO) enrichment analysis of differentially expressed genes between the Ctrl and LAN groups. There were significant differences in various biological processes. The size of each dot represents the proportion of genes in each process among all differentially expressed genes. red, more significant; blue, less significant.